

The Graph of Our Mind

Balázs Szalkai^a, Bálint Varga^a, Vince Grolmusz^{a,b,*}

^a*PIT Bioinformatics Group, Eötvös University, H-1117 Budapest, Hungary*

^b*Uratim Ltd., H-1118 Budapest, Hungary*

Abstract

Graph theory in the last two decades penetrated sociology, molecular biology, genetics, chemistry, computer engineering, and numerous other fields of science. One of the more recent areas of its applications is the study of the connections of the human brain. By the development of diffusion magnetic resonance imaging (diffusion MRI), it is possible today to map the connections between the 1-1.5 cm² regions of the gray matter of the human brain. These connections can be viewed as a graph: the vertices are the anatomically identified regions of the gray matter, and two vertices are connected by an edge if the diffusion MRI-based workflow finds neuronal fiber tracts between these areas. This way we can compute 1015-vertex graphs with tens of thousands of edges. In a previous work, we have analyzed the male and female braingraphs graph-theoretically, and we have found statistically significant differences in numerous parameters between the sexes: the female braingraphs are better expanders, have more edges, larger bipartition widths, and larger vertex cover than the braingraphs of the male subjects. Our previous study has applied the data of 96 subjects; here we present a much larger study of 426 subjects. Our data source is an NIH-founded project, the “Human Connectome Project (HCP)” public data release. As a service to the community, we have also made all of the braingraphs computed by us from the HCP data publicly available at the <http://braingraph.org> for independent validation and further investigations.

1. Introduction

It is an old dream to describe the neuronal-level braingraph (or connectome) of different organisms, where the vertices correspond to the neurons and two neurons are connected by an edge if there is a connection between them. The connectome of the roundworm *Caenorhabditis elegans* with 302 neurons was mapped 30 years ago [1], but larger braingraphs, especially the complete fruitfly *Drosophila melanogaster* braingraph (the “flybrain”) with approximately

*Corresponding author

Email addresses: szalkai@pitgroup.org (Balázs Szalkai), varga@pitgroup.org (Bálint Varga), grolmusz@pitgroup.org (Vince Grolmusz)

100,000 neurons remained unmapped in its entirety, despite using enormous resources and efforts worldwide. Mapping the connections in the human brain on the neuronal level is completely hopeless today, mostly because there are, on the average, 86 billion neurons in the human brain [2]. Constructing human braingraphs (or "connectomes"), where the vertices are not single neurons, but much larger areas of the gray matter of the brain (called Regions of Interest, ROIs), is possible, and it is the subject of a very intensive research work today. Two vertices, corresponding to the ROIs, are connected by an edge if a diffusion-MRI based workflow finds neuronal connections between them. In the process of the Human Connectome Project [3], an enormous amount of data and numerous tools were created related to the mapping of the human brain, and the resulting data were deposited in publicly available databases of dozens of terabytes.

Our focus in this work is the graph theoretical analysis of the connections of the brain; consequently, we just sketch the process of the construction of this graph here.

The human brain tissue, roughly, has two distinct parts: the white matter and the gray matter. The gray matter, by some simplifications, consists of the cell-bodies (or *somas*) of the neurons, and the white matter from the fibers of *axons* (long projections from the somas), insulated by lipid-like myelin sheaths. The cortex of the brain, and also some sub-cortical areas, contain gray matter, and most of the inner parts of the brain contain white matter. Again with some simplifications, the connections between the somas of the neurons, the axons, run in the white matter, except the very short axons running entirely in the gray matter.

Diffusion magnetic resonance imaging (MRI) is, again roughly speaking, capable of measuring the direction of the diffusion of the water molecules in living tissues, without any contrast material. The gray matter of the brain consists of the cell bodies (somas) of the neurons, consequently, there is no any distinguished direction of the diffusion of the water molecules in the somas: in each direction the molecules can move freely. In the white matter, however, the neuronal fibers consisted of long axons, so the water molecules move more easily and more probably in the direction of the axons than perpendicularly, through the cell membrane, bordering the axons. Therefore, in each point of a given axon in the white matter, the diffusion of the water molecules is larger in directions parallel to the axons and smaller in other directions.

This way one can distinguish the white matter and the gray matter of the brain (this step is called partitioning). Moreover, by following or tracking the directions of the stronger diffusion, it is possible to map the orbits of the neuronal fibers in the white matter (this step is called tractography). Certainly, when the fiber tracts are crossed, it is not easy to follow the correct directions of the axons.

After the tractography is performed, one gets an image, similar to Figure 1. Most of the fibers start and end on the surface — the cortex — of the brain.

We are interested in the connections between the gray matter areas, mostly of the cortical areas, and we ignore the exact orbits of the neuronal fibers in

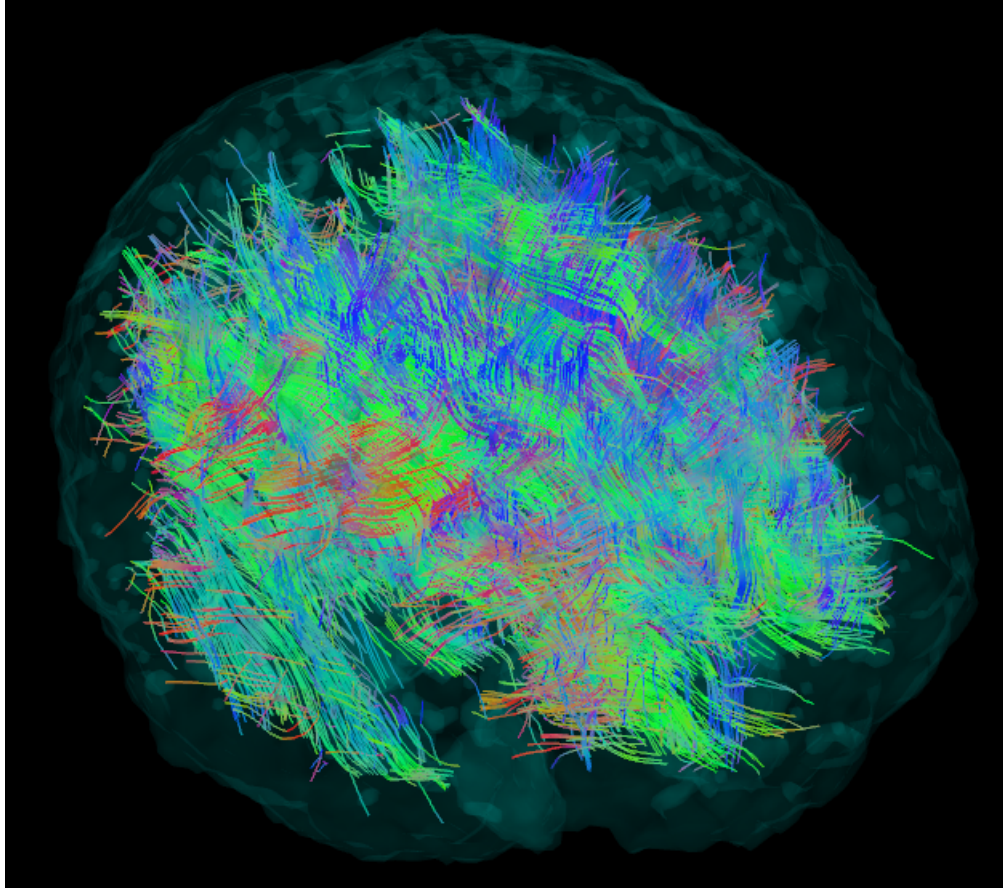


Figure 1: The result of the tractography phase. Note the fibers starting and ending on the outer surface, the cortex of the brain, which consists of gray matter. The fibers are tracked only in the anisotropic white matter.

the white matter. That is, it is not interesting for us that where the “wires” run, just the fact of the connections between the separate areas of the gray matter. Naturally, the length or the number of neuronal fibers, connecting the gray matter ROIs, can be included in the graph as different weight functions on the edges.

Consequently, we define the graph as follows: the vertices are the small anatomical areas of the gray matter (ROIs), and two ROIs are connected by an edge if in the tractography phase, at least, one fiber is tracked between these two ROIs. We are considering five different resolutions of ROIs, and also five different weight functions, computed from the properties of the fibers, connecting the ROIs.

2. Previous work

Numerous publications cover the connectome [4, 5] of healthy humans [6, 7, 8, 9] and also the connectomes of the healthy and the diseased brain [10, 11, 12, 13, 14]. Usually, these works analyze only 80-100 vertex graphs on the whole brain, and they are using concepts that originate from the network science, developed for large graphs of millions of vertices, found, e.g., in the graph of the World Wide Web.

Here we present another approach: We are analyzing larger graphs, up to 1015 vertices, and our algorithms are originated from graph theory and not from network science. In other words, we are also computing graph parameters that are quite hopeless to compute for graphs with millions of vertices.

In our previous work, we have made comparisons between the braingraphs of numerous subjects with several focuses:

- (i) We have constructed the Budapest Reference Connectome Server <http://connectome.pitgroup.org>, which generates the common edges of up to 477 graphs of 1015 vertices, according to selectable parameters [15, 16];
- (ii) We have compared the diversity of the edges in distinct cerebral areas in 392 individual brains in [17];
- (iii) Based on a feature of the Budapest Reference Connectome Server, we have found a probable connection between the consensus connectomes and the axon-development of the human brain [18].
- (iv) We have compared women’s and men’s connectomes in 96 subjects, and found that the braingraphs of females have numerous, statistically significant advantages in graph theoretical properties that are characteristic of the better connections [19].

The Budapest Reference Connectome Server <http://connectome.pitgroup.org> is also a good choice for the instant visualization of the braingraph.

3. Our results

In the present work we are considering a 426-subject dataset from the Human Connectome Project public release [3]. For each subject, we compute braingraphs with five different vertex-numbers: 83, 129, 234, 463 and 1015. The vertices correspond to anatomical areas of the gray matter in different resolutions.

The goal is to assign the same named vertex to the same anatomical region, in all the five resolutions, in the case of all subjects. Naturally, the size and the shape of the brain of all subjects differ; therefore it is a non-trivial task to assign the same nodes (or ROIs) to the same anatomical regions for all subjects. This is called the “registration problem”, and we have applied the

solution from the FreeSurfer suite of programs [20] that mapped the individual brains to the Desikan-Killiany brain atlas [21]. Roughly, the registration method applies homeomorphisms in order to correspond the major cortical patterns of *sulci* and *gyri* between individual cortices.

We were using five different resolutions in 83, 129, 234, 463 and 1015 vertices, because for smaller values the graph structure is poorer, and for the higher resolutions there is a possibility of the registration errors, due to the potentially too small areas corresponded to the vertices. Therefore, we have computed and analyzed the graph properties for all of these five resolutions, instead of deciding arbitrarily that one of the resolutions are the best for our goals.

For every graph, we have considered five different edge weights. Four of these describe some quantities, related to the neuronal fibers, defining the edge in question. More exactly, the weight functions are:

- **Unweighted:** Each edge has the same weight 1;
- **FiberN:** The number of fibers discovered in the tractography step between the nodes, corresponded to ROIs;
- **FAMean:** The average of the fractional anisotropies [22] of the neuronal fibers, connecting the endpoints of the edge;
- **FiberLengthMean:** The average fiber-lengths between the endpoints of the edge.
- **FiberNDivLength:** The number of fiber tracts connecting the end-nodes, divided by the mean length of those fibers.

The last weight function, **FiberNDivLength**, describes a conductance-like quantity in a very simple electrical model: the resistances is proportional to the average fiber length and inversely proportional to the number of wires connecting the endpoints. Similarly, it is also describing a reliability measure of the edge: longer fibers are less reliable due to tractography errors, but multiple fibers between the same ROIs are increasing the reliability.

Other authors have considered the number of edges (weighted or unweighted), running between pre-defined areas of the brain. One of the main focuses of these works was the ratio between the edges, running between the two hemispheres of the brain divided by the number of edges running within each hemisphere [23, 24]. The authors of [24] considered 95-node graphs, computed from 949 subjects of a publicly unavailable dataset, and found that, relatively, males have more intra-hemispheric edges while females have more inter-hemispheric edges.

We were interested — instead of simple edge-counting between pre-defined vertex-sets — in computing much more elaborate graph-theoretic parameters of the braingraphs.

More exactly, we have computed the following parameters, for each graph, similarly as in [19, 25]:

- Number of edges (**Sum**). The weighted version of this number is the sum of the weights of the edges in the graph.
- Normalized largest eigenvalue (**AdjLMaxDivD**): The largest eigenvalue of the generalized adjacency matrix, divided by the average degree of the graph. The adjacency matrix of an n -vertex graph is an $n \times n$ matrix, where a_{ij} is 1 if $\{v_i, v_j\}$ is an edge, and 0 otherwise. The generalized adjacency matrix contains the weight of edge $\{v_i, v_j\}$ in a_{ij} . The division by the average degree of the vertices is important since the largest eigenvalue is bounded by the average- and maximum degrees [26], so a dense graph has a big λ_{max} largest eigenvalue because of the larger average degree. Since the vertex numbers are fixed, the average degree is already defined by the sum of weights for each graph.
- Eigengap of the transition matrix (**PGEigengap**): The transition matrix P_G is defined by dividing the rows of the generalized adjacency matrix by the generalized degree of the node, where the generalized degree is the sum of the weights of the edges, incident to the vertex. A random walk on a graph can be characterized by the probabilities, for each i and j , of moving from vertex v_i to vertex v_j . These probabilities are the elements of transition matrix P_G , with all the row-sums equal to 1. The eigengap of a matrix is the difference between the largest and the second largest eigenvalue of P_G , and it is characteristic of the expander property of the graph: the larger the gap, the better expander is the graph (see [27]).
- Hoffman's bound (**HoffmanBound**): If λ_{max} and λ_{min} denote the largest and smallest eigenvalues of the adjacency matrix, then Hoffman's bound is defined as

$$1 + \frac{\lambda_{max}}{|\lambda_{min}|}.$$

This quantity is a lower estimation for the chromatic number of the graph.

- Logarithm of the number of the spanning forests (**LogAbsSpanningForestN**): The quantity of the spanning trees in a connected graph can be computed from the spectrum of its Laplacian [28, 29]. Graphs with more edges usually have more spanning trees, since the addition of an edge does not decrease the number of the spanning trees. For non-connected graphs, the number of spanning forests is the product of the numbers of the spanning trees of their components. The quantity **LogAbsSpanningForestN** is defined to be the logarithm of the number of spanning forests in the unweighted case. For other weight functions, if we define the weight of a tree by the product of the weights of its edges, then **LogAbsSpanningForestN** equals to the sum of the logarithms of the weights of the spanning trees in the forests.
- Balanced minimum cut, divided by the number of edges (**MinCutBalDivSum**): If the nodes of a graph are partitioned into

two classes, then a *cut* is the set of the edges running between these two classes. When we are looking for a *minimum cut* in a graph, most frequently one of the classes is small (say it contains just one vertex) and the other all the remaining vertices. Therefore, the most interesting case is when the sizes of the two classes of the partitions differ by at most one. Finding such a partition with the smallest cut is the "balanced minimum cut" or the "minimal bisection width" problem. This quantity, in a certain sense, describes the "bottleneck" of the graph, and it is an important characteristic of the interconnection networks (like the butterfly, the cube connected cycles, or the De Bruijn network, [30]) in computer engineering. For the whole brain graph, one may expect that the minimum cut corresponds to the partition to the two hemispheres, which was found when we analyzed the results. Consequently, this quantity is interesting *within* the hemispheres, when only the nodes of the right- or the left hemisphere is partitioned into two classes of equal size. Computing the balanced minimum cut is NP-hard [31], but its computation for the input-sizes of this study is possible with contemporary integer programming software. If we double every edge in a graph (allowing two edges between two vertices) then the minimum balanced cut will also be doubled. So, it is natural to expect that graphs with more edges may have larger minimum balanced cut just because the more edges present. However, if we *norm (i.e., divided by)* the balanced minimum cut with the number of the edges in the graph examined, then this effect can be factored out: for example, in the doubled-edge graph the balanced minimum cut is also doubled, but when its size is divided by the doubled edge number, the normed value will be the same as in the original graph. So, when `MinCutBalDivSum` is considered, the effects of the edge-numbers are factored out.

- Minimum cost spanning tree (`MinSpanningForest`), computed with Kruskal's algorithm [32].
- Minimum weighted vertex cover (`MinVertexCover`): We need to assign to each vertex a non-negative weight satisfying that for each edge, the sum of the weights of its two endpoints is at least 1. This is the relaxation of the NP-hard vertex-cover problem [33], since here we allow fractional weights, too. The sum of all vertex-weights with this constraint can be minimized in polynomial time by linear programming.
- Minimum vertex cover (`MinVertexCoverBinary`): Same as the quantity above, but the weights need to be 0 or 1. Alternatively, this number gives the size of the smallest vertex-set such that each edge is connected to at least one of the vertices in the set. This graph parameter is NP-hard, and we computed it only for the unweighted case by an integer programming (IP) solver SCIP <http://scip.zib.de> [34, 35].
- Maximum matching (`MaxMatching`): A graph matching is a set of edges without common vertices. A maximum matching contains the largest

number of edges. A maximum matching in a weighted graph is the matching with the maximum sum of weights taken on its edges.

- Maximum fractional matching (**MaxFracMatching**): is the linear-programming relaxation of the maximum matching problem. In the unweighted case, non-negative values $x(e)$ are searched for each edge e in the graph, satisfying that for each vertex v in the graph, the sum of $x(e)$ -s for the edges that are incident to v is at most 1. The maximum of the sums of $\sum_e x(e)$ is the maximum fractional matching for a graph. For the weighted version with weight function w , $\sum_e x(e)w(e)$ needs to be maximized.
- The sum of the weights of the edges in the left hemisphere, divided by the sum of the weights of the edges in the right hemisphere (**LeftRatio**).
- (**OutBasalGanglia**, **OutBrainstem**, **OutFrontal**, **OutInsula**, **OutLimbic**, **OutOccipital**, **OutParietal**, **OutTemporal**, **OutThalamus**) These quantities give the sum of the weights of the edges, crossing the border of the cerebral lobes noted.

The above parameters were computed for all five resolutions and the left and the right hemispheres and also for the whole connectome, with all five weight functions (with the following exceptions: **MinVertexCoverBinary** was computed only for the unweighted case, and the **MinSpanningTree** was not computed for the unweighted case, and **LeftRatio** was computed only for the whole brain).

The results, for each subject, each resolution and each weight function are detailed in a large Excel table, downloadable from the site <http://uratim.com/bigtableB.zip>.

3.1. The syntactics of the results:

Each parameter-name in the table at <http://uratim.com/bigtableB.zip> and elsewhere in this work contains two separating “_” symbols that define three parts of the name. The first part describes the hemisphere or the whole connectome with the words Left, Right or All. The second part describes the parameter computed, and the third part the weight function used. For example, **All_AdjLMaxDivD_FiberNDivLength** means that the normalized largest eigenvalue **AdjLMaxDivD** was computed for the whole brain, with the **FiberNDivLength** weight function (see above).

In the Table <http://uratim.com/bigtableB.zip>, the first column, round index is used in the statistical analysis. Second column, “id”, is the anonymized subject ID of the Human Connectome Project’s 500-subject public release. Column 3 gives the sex of the subject, 0: female, 1: male. Fourth column gives the age-groups 0: 22-25 years; 1: 26-30 years; 2: 31-35 years; 3: 35+ years. Column 5 gives the number of vertices of the graph analyzed.

3.2. The analysis of the results:

The data that we used from the public release of the Human Connectome project, contains diffusion MRI recordings from healthy male and female subjects of age 22 through 35. Therefore, if we want to find correlations of the graph theoretical characteristics of the connectomes with some biological properties, we may easily use either the sex or the age of the subjects.

Our main finding now, on a large data set, validates our earlier results that was made on a much smaller data set in [19]: in numerous graph theoretical parameters, women’s connectomes show statistically significant advantages against the men’s respective parameters. The parameters in question are related to “better connectivity” in several aspects.

In the Appendix, we are enclosing several large tables with the results. In Table 1, the results of statistical analysis are detailed: the parameters with the bold last column are *all* significantly differ between the female and the male connectomes: the vast majority is “better” for the females. If the last column is not bold, but the fifth column is typeset in italic then those parameters, one-by-one, significantly differ between the sexes, but it is unlikely that all of them differ significantly (type II statistical errors are possible).

For example, as it is seen in Table 1, differences in the **PGEigengap** values show the better expander property in the braingraph of the females, in both hemispheres. The differences in the **Sum** quantity shows that in both hemispheres, women have more edges than men, and this statement remains true for weighted edges with most weight functions. Very strong statistical evidence show the difference and the women’s advantage in the edge-number normalized balanced minimum cut in the left hemisphere. Matching numbers (both fractional and integer) are also significantly larger in the case of females.

Seemingly, in the left hemisphere the women’s advantage is stronger in several parameters: the first several rows of Table 1 contains mostly “Left” or “All” prefixes in the second column.

In very few cases men have better parameters: e.g., in resolution 83, **All_MinSpanningForest_FiberLengthMean** is significantly larger for men than for women. Similarly, another parameter, weighted by **FiberLengthMean**, the **All_MinSpanningForest_FiberLengthMean** in 234-resolution is also larger for males. We believe that the larger brain size with the **FiberLengthMean** weighting compensates the fewer connections of the males in these cases.

In the Appendix, we are also enclosing Tables 2, 3, 4, 5 and 6 that give the detailed averaged results for each resolution for each graph parameter with ANOVA statistical analysis. The subject-level data are also available at <http://uratic.com/bigtableB.zip>.

4. Computational details and data availability

We have used the Connectome Mapper Toolkit [36] <http://cmtk.org> for brain tissue segmentation into gray and white matter, partitioning the brain into anatomical regions, for tractography (tracking the axonal fibers in the

white matter) and for the construction of the graphs from the fibers identified in the tractography phase of the workflow. The partitioning was based on the FreeSurfer suite of programs [20], according to the Desikan-Killiany brain anatomy atlas [21]. The tractography used the MRtrix processing tool [37] with randomized seeding and with the deterministic streamline method.

The graphs were constructed using the results of the tractography step: two nodes, corresponding to ROIs, were connected if there existed, at least one, fiber connecting them. Loops were deleted from the graph.

Graph parameters were computed by the integer programming (IP) solver SCIP <http://scip.zib.de>, [34, 35], and by some in-house scripts.

The unprocessed and pre-processed MRI data is available at the Human Connectome Project’s website: <http://www.humanconnectome.org/documentation/S500> [3]. The assembled graphs that we analyzed in the present work can be downloaded at the site <http://braingraph.org/download-pit-group-connectomes/>. The individual graph results are detailed in a large Excel table at the site <http://uratim.com/bigtableB.zip>

4.1. Statistical analysis

Our statistical null-hypothesis [38] was that the graph parameters do not differ between males and females. For dealing with both type I and type II statistical errors, we have partitioned the subjects into classes quasi-randomly: subjects with IDs with even digit-sums went to group 0, and those with odd digit sums went to group 1 (c.f. the first column of <http://uratim.com/bigtableB.zip>).

We applied group 0 for a base set, for making hypotheses, and group 1 as a holdout set, for testing those hypotheses. The hypotheses on group 0 were filtered by “Analysis of variance” (ANOVA) [39]: only the hypotheses with p-value of less than 1% were selected for the testing in the holdout set. Next, the selected hypotheses were tested on group 1, with the rather strict Holm-Bonferroni correction method [40]. The significance level in the Holm-Bonferroni correction was set to 5%.

4.2. Handling possible artifacts

While we have applied the same computational workflow for the data of the both sexes, it is still possible that some non-sex specific artifact caused the significant differences in the graph parameters between men and women subjects. One possible cause may be the statistical difference between the size of the brain of the sexes [41]. In the tractography step, it may happen that the longer neural fibers of the males cannot be tracked so reliably as the shorter fibers of the females. To close out this possible error, we have selected 36 small-brain males and 36 large-brain females such that all the females have larger brains than all the males in the data set [25]. Next, we have computed the graph theoretical parameters as in the present work. Two main findings of ours were: (i) the small-brain men did not have the advantages identified in the set of the women in the present study; (ii) in several parameters, mostly with the

weight function **FAMean**, women still have the statistically significant advantages identified in the present study.

We find this result decisive that the graph-theoretical differences in the connectomes are due to sex differences and not size differences.

5. Acknowledgments

Data were provided in part by the Human Connectome Project, WU-Minn Consortium (Principal Investigators: David Van Essen and Kamil Ugurbil; 1U54MH091657) funded by the 16 NIH Institutes and Centers that support the NIH Blueprint for Neuroscience Research; and by the McDonnell Center for Systems Neuroscience at Washington University.

6. References

References

- [1] J. White, E. Southgate, J. Thomson, S. Brenner, The structure of the nervous system of the nematode *Caenorhabditis elegans*: the mind of a worm, *Phil. Trans. R. Soc. Lond* 314 (1986) 1–340.
- [2] F. A. Azevedo, L. R. Carvalho, L. T. Grinberg, J. M. Farfel, R. E. Ferretti, R. E. Leite, R. Lent, S. Herculano-Houzel, et al., Equal numbers of neuronal and nonneuronal cells make the human brain an isometrically scaled-up primate brain, *Journal of Comparative Neurology* 513 (5) (2009) 532–541.
- [3] J. A. McNab, B. L. Edlow, T. Witzel, S. Y. Huang, H. Bhat, K. Heberlein, T. Feiweier, K. Liu, B. Keil, J. Cohen-Adad, M. D. Tisdall, R. D. Folkerth, H. C. Kinney, L. L. Wald, The Human Connectome Project and beyond: initial applications of 300 mT/m gradients., *Neuroimage* 80 (2013) 234–245. doi:10.1016/j.neuroimage.2013.05.074.
URL <http://dx.doi.org/10.1016/j.neuroimage.2013.05.074>
- [4] P. Hagmann, P. E. Grant, D. A. Fair, Mr connectomics: a conceptual framework for studying the developing brain., *Front Syst Neurosci* 6 (2012) 43. doi:10.3389/fnsys.2012.00043.
URL <http://dx.doi.org/10.3389/fnsys.2012.00043>
- [5] R. C. Craddock, M. P. Milham, S. M. LaConte, Predicting intrinsic brain activity., *Neuroimage* 82 (2013) 127–136. doi:10.1016/j.neuroimage.2013.05.072.
URL <http://dx.doi.org/10.1016/j.neuroimage.2013.05.072>
- [6] G. Ball, P. Aljabar, S. Zebari, N. Tusor, T. Arichi, N. Merchant, E. C. Robinson, E. Ogundipe, D. Rueckert, A. D. Edwards, S. J. Counsell, Rich-club organization of the newborn human brain., *Proc Natl Acad Sci U S A* 111 (20) (2014) 7456–7461. doi:10.1073/pnas.1324118111.
URL <http://dx.doi.org/10.1073/pnas.1324118111>

- [7] C. I. Bargmann, Beyond the connectome: how neuromodulators shape neural circuits., *Bioessays* 34 (6) (2012) 458–465. doi:10.1002/bies.201100185.
URL <http://dx.doi.org/10.1002/bies.201100185>
- [8] D. Batalle, E. Muñoz-Moreno, F. Figueras, N. Bargallo, E. Eixarch, E. Gratacos, Normalization of similarity-based individual brain networks from gray matter MRI and its association with neurodevelopment in infants with intrauterine growth restriction., *Neuroimage* 83 (2013) 901–911. doi:10.1016/j.neuroimage.2013.07.045.
URL <http://dx.doi.org/10.1016/j.neuroimage.2013.07.045>
- [9] D. J. Graham, Routing in the brain., *Front Comput Neurosci* 8 (2014) 44. doi:10.3389/fncom.2014.00044.
URL <http://dx.doi.org/10.3389/fncom.2014.00044>
- [10] F. Agosta, S. Galantucci, P. Valsasina, E. Canu, A. Meani, A. Marcone, G. Magnani, A. Falini, G. Comi, M. Filippi, Disrupted brain connectome in semantic variant of primary progressive aphasia., *Neurobiol Aging* doi:10.1016/j.neurobiolaging.2014.05.017.
URL <http://dx.doi.org/10.1016/j.neurobiolaging.2014.05.017>
- [11] A. F. Alexander-Bloch, P. T. Reiss, J. Rapoport, H. McAdams, J. N. Giedd, E. T. Bullmore, N. Gogtay, Abnormal cortical growth in schizophrenia targets normative modules of synchronized development., *Biol Psychiatry* doi:10.1016/j.biopsych.2014.02.010.
URL <http://dx.doi.org/10.1016/j.biopsych.2014.02.010>
- [12] J. T. Baker, A. J. Holmes, G. A. Masters, B. T. T. Yeo, F. Krienen, R. L. Buckner, D. Öngür, Disruption of cortical association networks in schizophrenia and psychotic bipolar disorder., *JAMA Psychiatry* 71 (2) (2014) 109–118. doi:10.1001/jamapsychiatry.2013.3469.
URL <http://dx.doi.org/10.1001/jamapsychiatry.2013.3469>
- [13] P. Besson, V. Dinkelacker, R. Valabregue, L. Thivard, X. Leclerc, M. Baulac, D. Sammler, O. Colliot, S. Lehericy, S. Samson, S. Dupont, Structural connectivity differences in left and right temporal lobe epilepsy., *Neuroimage* 100C (2014) 135–144. doi:10.1016/j.neuroimage.2014.04.071.
URL <http://dx.doi.org/10.1016/j.neuroimage.2014.04.071>
- [14] L. Bonilha, T. Nesland, C. Rorden, P. Fillmore, R. P. Ratnayake, J. Fridriksson, Mapping remote subcortical ramifications of injury after ischemic strokes., *Behav Neurol* 2014 (2014) 215380. doi:10.1155/2014/215380.
URL <http://dx.doi.org/10.1155/2014/215380>
- [15] B. Szalkai, C. Kerepesi, B. Varga, V. Grolmusz, The Budapest Reference Connectome Server v2. 0, *Neuroscience Letters* 595 (2015) 60–62.

- [16] B. Szalkai, C. Kerepesi, B. Varga, V. Grolmusz, Parameterizable consensus connectomes from the human connectome project: The budapest reference connectome server v3.0, arXiv preprint arXiv:1602.04776arXiv:1602.04776.
- [17] C. Kerepesi, B. Szalkai, B. Varga, V. Grolmusz, Comparative connectomics: Mapping the inter-individual variability of connections within the regions of the human brain, arXiv preprint arXiv:1507.00327.
- [18] C. Kerepesi, B. Szalkai, B. Varga, V. Grolmusz, Does the budapest reference connectome server shed light to the development of the connections of the human brain?, arXiv preprint arXiv:1509.05703.
- [19] B. Szalkai, B. Varga, V. Grolmusz, Graph theoretical analysis reveals: Women’s brains are better connected than men’s., PLoS One 10 (7) (2015) e0130045. doi:10.1371/journal.pone.0130045.
URL <http://dx.doi.org/10.1371/journal.pone.0130045>
- [20] B. Fischl, Freesurfer, Neuroimage 62 (2) (2012) 774–781.
- [21] R. S. Desikan, F. Ségonne, B. Fischl, B. T. Quinn, B. C. Dickerson, D. Blacker, R. L. Buckner, A. M. Dale, R. P. Maguire, B. T. Hyman, M. S. Albert, R. J. Killiany, An automated labeling system for subdividing the human cerebral cortex on mri scans into gyral based regions of interest., Neuroimage 31 (3) (2006) 968–980. doi:10.1016/j.neuroimage.2006.01.021.
URL <http://dx.doi.org/10.1016/j.neuroimage.2006.01.021>
- [22] P. J. Basser, C. Pierpaoli, Microstructural and physiological features of tissues elucidated by quantitative-diffusion-tensor mri., J Magn Reson 213 (2) (1996) 560–570. doi:10.1016/j.jmr.2011.09.022.
URL <http://dx.doi.org/10.1016/j.jmr.2011.09.022>
- [23] N. Jahanshad, I. Aganj, C. Lenglet, A. Joshi, Y. Jin, M. Barysheva, K. L. McMahon, G. De Zubicaray, N. G. Martin, M. J. Wright, et al., Sex differences in the human connectome: 4-tesla high angular resolution diffusion imaging (hardi) tractography in 234 young adult twins, in: Biomedical Imaging: From Nano to Macro, 2011 IEEE International Symposium on, IEEE, 2011, pp. 939–943.
- [24] M. Ingalhalikar, A. Smith, D. Parker, T. D. Satterthwaite, M. A. Elliott, K. Ruparel, H. Hakonarson, R. E. Gur, R. C. Gur, R. Verma, Sex differences in the structural connectome of the human brain., Proc Natl Acad Sci U S A 111 (2) (2014) 823–828. doi:10.1073/pnas.1316909110.
URL <http://dx.doi.org/10.1073/pnas.1316909110>
- [25] B. Szalkai, B. Varga, V. Grolmusz, The advantage is at the ladies: Brain size bias-compensated graph-theoretical parameters are also better in women’s connectomes, arXiv preprint arXiv:1512.01156.

- [26] L. Lovasz, Eigenvalues of graphs, Tech. rep., Department of Computer Science, Eotvos University, Pazmany Peter 1/C, H-1117 Budapest, Hungary (November 2007).
URL <http://www.cs.elte.hu/~lovasz/eigenvals-x.pdf>
- [27] S. Hoory, N. Linial, A. Wigderson, Expander graphs and their applications, *Bulletin of the American Mathematical Society* 43 (4) (2006) 439–561.
- [28] G. Kirchhoff, Über die Auflösung der Gleichungen, auf welche man bei der Untersuchung der linearen Vertheilung galvanischer Ströme geführt wird, *Ann. Phys. Chem.* 72 (12) (1847) 497–508.
- [29] F. R. Chung, *Spectral graph theory*, Vol. 92, American Mathematical Soc., 1997.
- [30] R. E. Tarjan, *Data structures and network algorithms*, Vol. 44 of CBMS-NSF Regional Conference Series in Applied Mathematics, Society for Industrial Applied Mathematics, 1983.
- [31] M. R. Garey, D. S. Johnson, L. Stockmeyer, Some simplified NP-complete graph problems, *Theoretical computer science* 1 (3) (1976) 237–267.
- [32] E. L. Lawler, *Combinatorial optimization: networks and matroids*, Courier Dover Publications, 1976.
- [33] D. S. Hochbaum, Approximation algorithms for the set covering and vertex cover problems, *SIAM Journal on Computing* 11 (3) (1982) 555–556.
- [34] T. Achterberg, T. Berthold, T. Koch, K. Wolter, Constraint integer programming: A new approach to integrate CP and MIP, in: *Integration of AI and OR techniques in constraint programming for combinatorial optimization problems*, Springer, 2008, pp. 6–20.
- [35] T. Achterberg, SCIP: solving constraint integer programs, *Mathematical Programming Computation* 1 (1) (2009) 1–41.
- [36] A. Daducci, S. Gerhard, A. Griffa, A. Lemkaddem, L. Cammoun, X. Gignandet, R. Meuli, P. Hagmann, J.-P. Thiran, The connectome mapper: an open-source processing pipeline to map connectomes with MRI., *PLoS One* 7 (12) (2012) e48121. doi:10.1371/journal.pone.0048121.
URL <http://dx.doi.org/10.1371/journal.pone.0048121>
- [37] J. Tournier, F. Calamante, A. Connelly, et al., Mrtrix: diffusion tractography in crossing fiber regions, *International Journal of Imaging Systems and Technology* 22 (1) (2012) 53–66.
- [38] P. G. Hoel, *Introduction to mathematical statistics.*, 5th Edition, John Wiley & Sons, Inc., New York, 1984.
- [39] T. H. Wonnacott, R. J. Wonnacott, *Introductory statistics*, Vol. 19690, Wiley New York, 1972.

- [40] S. Holm, A simple sequentially rejective multiple test procedure, Scandina-
vian Journal of Statistics (1979) 65–70.
- [41] S. F. Witelson, H. Beresh, D. L. Kigar, Intelligence and brain size in 100
postmortem brains: sex, lateralization and age factors., Brain 129 (Pt 2)
(2006) 386–398. doi:10.1093/brain/awh696.
URL <http://dx.doi.org/10.1093/brain/awh696>

7. Appendix

7.1. Table 1:

Table 1: The results and the statistical analysis of the graph-theoretical evaluation of the sex differences in the 426-subject data set. The first column gives the resolutions: the number of vertices in the whole graph. The second column describes the graph parameter computed: its syntactics is as follows: each parameter-name contains two separating “.” symbols that define three parts of the parameter-name. The first part describe the hemisphere or the whole connectome with the words Left, Right or All. The second part describes the parameter computed, and the third part the weight function used. The third column contains values of the parameters, averaged to the sexes. The fourth column describes the p-values of the first round, the fifth column the p-values of the second round, and the sixth column the (very strict) Holm-Bonferroni correction of the p-value. With $p=0.05$ all the rows with boldface last column describe significantly different graph theoretical properties between sexes. One-by-one, each row with italic fifth column describe significant differences between sexes, with $p=0.05$. For the details, we refer to the section “Statistical analysis”.

Scale	Property	Female Male	p (1st)	p (2nd)	p (corrected)
129	Left_PGEigengap_FiberNDivLength	0.0948 0.0811	0.00000	<i>0.00000</i>	0.00000
234	Left_PGEigengap_FiberNDivLength	0.0712 0.0606	0.00000	<i>0.00000</i>	0.00000
129	Left_PGEigengap_FiberN	0.1219 0.1007	0.00000	<i>0.00000</i>	0.00000
83	Left_PGEigengap_FiberNDivLength	0.1412 0.1249	0.00000	<i>0.00000</i>	0.00000
234	Left_PGEigengap_FiberN	0.0946 0.0782	0.00000	<i>0.00000</i>	0.00000
83	Left_PGEigengap_FiberN	0.1675 0.1430	0.00000	<i>0.00000</i>	0.00000
234	All_PGEigengap_FiberNDivLength	0.0242 0.0201	0.00000	<i>0.00000</i>	0.00000
83	Left_MinCutBalDivSum_FiberNDivLength	0.1320 0.1186	0.00000	<i>0.00000</i>	0.00000
83	All_LogSpanningForestN_FiberNDivLength	147.7706 142.7239	0.00000	<i>0.00000</i>	0.00000
83	Left_MinCutBalDivSum_FiberN	0.1305 0.1151	0.00000	<i>0.00000</i>	0.00000
129	All_PGEigengap_FiberNDivLength	0.0284 0.0237	0.00000	<i>0.00000</i>	0.00000
83	All_Sum_FiberN	11072.8196 10547.3855	0.00000	<i>0.00000</i>	0.00000
129	Left_MinCutBalDivSum_FiberN	0.1223 0.1052	0.00000	<i>0.00000</i>	0.00000
83	All_PGEigengap_FiberNDivLength	0.0346 0.0291	0.00000	<i>0.00000</i>	0.00000
83	Left_Sum_Unweighted	282.0573 269.7710	0.00000	<i>0.00000</i>	0.00001
234	Left_MinCutBalDivSum_FiberN	0.0995 0.0864	0.00000	<i>0.00000</i>	0.00002
83	All_Sum_FAMean	218.7173 202.2306	0.00000	<i>0.00000</i>	0.00002
463	Left_MinCutBalDivSum_FiberN	0.0702 0.0608	0.00000	<i>0.00000</i>	0.00002
129	All_Sum_FiberN	12238.966 11779.5060	0.00000	<i>0.00000</i>	0.00003
83	Left_LogSpanningForestN_FiberNDivLength	73.9377 71.1251	0.00001	<i>0.00000</i>	0.00003
234	Left_PGEigengap_Unweighted	0.1282 0.1104	0.00000	<i>0.00000</i>	0.00004
83	All_LogSpanningForestN_FAMean	109.3931 102.6911	0.00000	<i>0.00000</i>	0.00005
83	All_Sum_Unweighted	564.4098 544.3012	0.00000	<i>0.00000</i>	0.00006
83	Left_Sum_FAMean	105.9875 97.2824	0.00000	<i>0.00000</i>	0.00006
129	Left_PGEigengap_Unweighted	0.2047 0.1774	0.00000	<i>0.00000</i>	0.00006
463	Left_MinCutBalDivSum_Unweighted	0.0927 0.0805	0.00000	<i>0.00000</i>	0.00007
234	All_PGEigengap_FiberN	0.0250 0.0212	0.00000	<i>0.00000</i>	0.00007
129	All_LogSpanningForestN_FiberNDivLength	210.3350 204.5640	0.00000	<i>0.00000</i>	0.00007
83	Left_LogSpanningForestN_FAMean	53.1346 49.1865	0.00000	<i>0.00000</i>	0.00008
83	Left_PGEigengap_Unweighted	0.3083 0.2769	0.00000	<i>0.00000</i>	0.00010
83	Left_MinCutBalDivSum_FAMean	0.24907 0.2279	0.00001	<i>0.00000</i>	0.00013
129	Left_PGEigengap_FAMean	0.2286 0.1995	0.00000	<i>0.00000</i>	0.00014
129	All_PGEigengap_FiberN	0.0277 0.0236	0.00000	<i>0.00000</i>	0.00016

463	Left_MinCutBalDivSum_FiberLengthMean	0.0960 0.0810	0.00002	0.00000	0.00023
83	Left_PGEigengap_FAMean	0.3364 0.3026	0.00000	0.00000	0.00023
83	Left_MinCutBalDivSum_Unweighted	0.2448 0.2266	0.00000	0.00000	0.00029
83	All_PGEigengap_FiberN	0.0317 0.0272	0.00000	0.00000	0.00029
83	All_Sum_FiberNDivLength	471.6398 448.0170	0.00000	0.00000	0.00029
83	Right_Sum_FiberN	5273.6065 5044.8072	0.00000	0.00000	0.00030
234	All_Sum_FiberN	13150.0833 12735.7590	0.00000	0.00000	0.00031
234	Left_MinCutBalDivSum_FiberLengthMean	0.1466 0.1258	0.00000	0.00000	0.00037
129	Left_MinCutBalDivSum_Unweighted	0.1929 0.1755	0.00000	0.00000	0.00042
83	Left_Sum_FiberN	5457.7213 5215.3012	0.00000	0.00000	0.00053
234	Left_PGEigengap_FAMean	0.1445 0.1263	0.00000	0.00000	0.00054
83	Left_LogSpanningForestN_Unweighted	95.2838 93.4346	0.00117	0.00000	0.00061
83	All_LogSpanningForestN_FiberN	396.1740 392.13187	0.00000	0.00000	0.00063
83	Right_Sum_FAMean	103.2289 96.5212	0.00000	0.00000	0.00066
129	All_Sum_FAMean	388.6029 363.4251	0.00000	0.00000	0.00071
234	Left_MinCutBalDivSum_Unweighted	0.1402 0.1265	0.00000	0.00000	0.00104
463	All_Sum_FiberN	13517.1239 13136.1445	0.00000	0.00000	0.00127
129	Left_LogSpanningForestN_FiberNDivLength	105.4555 102.2015	0.00023	0.00001	0.00150
234	Left_PGEigengap_FiberLengthMean	0.1495 0.1285	0.00000	0.00001	0.00175
129	All_LogSpanningForestN_FAMean	191.1538 182.0234	0.00000	0.00001	0.00198
129	Left_Sum_FiberN	6036.5583 5814.3373	0.00000	0.00001	0.00212
129	Right_HoffmanBound_FiberNDivLength	2.6708 2.5903	0.00255	0.00001	0.00219
1015	All_Sum_FiberN	13707.0416 13336.9397	0.00000	0.00001	0.00251
129	Left_MinCutBalDivSum_FiberLengthMean	0.1986 0.1774	0.00001	0.00001	0.00321
129	Right_Sum_FAMean	186.3736 174.8309	0.00000	0.00001	0.00332
234	Right_PGEigengap_FiberNDivLength	0.0702 0.0639	0.00000	0.00001	0.00370
83	Left_MinCutBalDivSum_FiberLengthMean	0.2368 0.2154	0.00003	0.00002	0.00421
1015	Left_MinCutBalDivSum_Unweighted	0.0566 0.0497	0.00000	0.00002	0.00455
83	Right_LogSpanningForestN_FiberNDivLength	69.2438 67.3483	0.00000	0.00002	0.00526
463	All_MinSpanningForest_FAMean	97.8528 93.9407	0.00000	0.00002	0.00557
234	All_MinSpanningForest_FAMean	51.1676 48.9654	0.00000	0.00002	0.00572
129	Right_MinVertexCover_FAMean	14.6370 14.1708	0.00009	0.00002	0.00589
129	Left_PGEigengap_FiberLengthMean	0.2354 0.2048	0.00001	0.00003	0.00627
129	Left_Sum_FAMean	192.6335 180.2677	0.00000	0.00003	0.00659
83	All_MaxMatching_FAMean	18.4793 17.8628	0.00000	0.00003	0.00678
234	All_Sum_FAMean	674.3861 637.7626	0.00000	0.00003	0.00740
129	All_MinVertexCover_FAMean	29.2681 28.3448	0.00000	0.00003	0.00769
129	Right_PGEigengap_Unweighted	0.2018 0.1819	0.00000	0.00003	0.00796
83	Left_LogSpanningForestN_FiberN	198.7272 196.5478	0.00045	0.00003	0.00813
129	Right_Sum_FiberN	5865.325 5675.9036	0.00000	0.00004	0.00914
83	Right_LogSpanningForestN_FAMean	51.1770 48.6093	0.00000	0.00004	0.00915
129	All_LogSpanningForestN_FiberN	597.6881 592.8658	0.00000	0.00004	0.00918
129	Right_LogSpanningForestN_FAMean	91.9198 87.7893	0.00000	0.00004	0.00916
129	Right_PGEigengap_FiberNDivLength	0.0904 525.9763	0.00000	0.00004	0.00925
1015	Left_MinCutBalDivSum_FiberLengthMean	0.0580 0.0500	0.00197	0.00004	0.00945
83	Right_Sum_FiberNDivLength	222.8988 213.3314	0.00000	0.00004	0.00973
83	Left_MinSpanningForest_FiberLengthMean	554.2756 567.6656	0.00146	0.00004	0.00971
83	All_LogSpanningForestN_Unweighted	191.0620 188.5304	0.00004	0.00005	0.01204
129	All_MinSpanningForest_FAMean	30.0726 28.5907	0.00000	0.00006	0.01351
83	Left_Sum_FiberNDivLength	232.2089 221.4498	0.00000	0.00006	0.01385
129	All_MinSpanningForest_FiberLengthMean	1642.1057 1666.9289	0.00007	0.00006	0.01431
129	Right_MinSpanningForest_FAMean	15.5645 14.7611	0.00009	0.00006	0.01447
83	Right_MinSpanningForest_FAMean	10.2995 9.6958	0.00019	0.00007	0.01516
129	Left_LogSpanningForestN_FAMean	94.4372 89.6353	0.00000	0.00007	0.01539
129	Left_MinSpanningForest_FiberLengthMean	826.0336 841.6138	0.00016	0.00007	0.01552
234	Right_MinSpanningForest_FAMean	25.9870 24.8290	0.00008	0.00007	0.01684
234	Right_MinVertexCover_FAMean	25.6497 24.9170	0.00019	0.00008	0.01794
83	All_MaxFracMatching_FAMean	18.5112 17.9306	0.00000	0.00008	0.01795
83	All_MinVertexCover_FAMean	18.5112 17.9306	0.00000	0.00008	0.01787
129	All_Sum_Unweighted	1008.0166 979.3975	0.00000	0.00008	0.01801
83	Right_MaxFracMatching_FAMean	9.2021 8.9143	0.00004	0.00008	0.01872
83	Right_MinVertexCover_FAMean	9.2021 8.9143	0.00004	0.00008	0.01864
463	Right_MinSpanningForest_FAMean	50.4171 48.29781	0.00005	0.00009	0.01997
83	Right_PGEigengap_Unweighted	0.2970 0.2748	0.00000	0.00009	0.01995
234	Left_Sum_FAMean	332.9738 314.1271	0.00000	0.00010	0.02095
129	Right_PGEigengap_FAMean	0.2242 0.2037	0.00000	0.00010	0.02190
83	Right_MaxMatching_FAMean	9.1786 8.8951	0.00003	0.00011	0.02264
83	All_MinSpanningForest_FAMean	19.7614 18.7034	0.00000	0.00011	0.02368

234	Left_Sum_FiberN	6532.7 6335.9879	0.00000	0.00012	0.02604
83	All_MinCutBalDivSum_FiberNDivLength	0.03410 0.0289	0.00000	0.00013	0.02719
83	Left_PGEigengap_FiberLengthMean	0.3342 0.3015	0.00000	0.00013	0.02760
83	Right_PGEigengap_FiberNDivLength	0.1480 0.1383	0.00000	0.00014	0.02852
234	Left_MinSpanningForest_FiberLengthMean	1424.5320 1442.5840	0.00028	0.00015	0.03074
234	All_MinVertexCover_FAMean	51.3348 49.8970	0.00000	0.00015	0.03086
234	Right_Sum_FAMean	331.7349 314.9959	0.00000	0.00015	0.03164
83	All_MinSpanningForest_FiberLengthMean	1093.0591 1111.8064	0.00017	0.00016	0.03371
129	Left_LogSpanningForestN_FiberN	300.1093 297.3925	0.00100	0.00018	0.03788
129	Right_LogSpanningForestN_FiberNDivLength	100.2820 98.0429	0.00009	0.00020	0.04110
1015	Left_MinCutBalDivSum_FiberN	0.0479 0.0432	0.00107	0.00021	0.04237
129	Left_Sum_Unweighted	510.8916 496.0602	0.00000	0.00022	0.04374
234	Right_PGEigengap_Unweighted	0.1194 0.1079	0.00000	0.00022	0.04430
129	All_HoffmanBound_Unweighted	4.5868 4.5055	0.00004	0.00023	0.04511
234	All_Sum_FiberNDivLength	617.1686 598.9007	0.00000	0.00024	0.04709
129	Right_HoffmanBound_Unweighted	4.6124 4.5159	0.00001	0.00028	0.05587
129	Right_MinCutBalDivSum_FiberLengthMean	0.1915 0.1753	0.00000	0.00035	0.06880
463	Right_AdjLMaxDivD_Unweighted	1.7949 1.7560	0.00152	0.00037	0.07193
1015	Right_AdjLMaxDivD_Unweighted	2.7110 2.6336	0.00147	0.00037	0.07307
83	Right_PGEigengap_FAMean	0.3247 0.3030	0.00000	0.00043	0.08256
463	Left_Sum_FiberN	6705.2396 6524.7228	0.00001	0.00043	0.08268
83	Left_AdjLMaxDivD_FAMean	1.3330 1.3538	0.00276	0.00043	0.08304
1015	Right_HoffmanBound_FiberN	2.3184 2.2759	0.00008	0.00046	0.08753
129	Right_HoffmanBound_FiberN	2.6444 2.5628	0.00010	0.00046	0.08723
234	Right_PGEigengap_FiberN	0.0909 0.0825	0.00000	0.00048	0.09081
129	Left_Sum_FiberNDivLength	269.5839 259.7618	0.00014	0.00048	0.09059
234	Right_Sum_FiberN	6272.2333 6109.0240	0.00000	0.00049	0.09082
234	All_LogSpanningForestN_FiberNDivLength	262.4479 256.2612	0.00295	0.00049	0.09065
463	All_Sum_FAMean	1019.7387 973.3478	0.00000	0.00052	0.09572
83	Right_MinCutBalDivSum_Unweighted	0.2377 0.2254	0.00000	0.00058	0.10656
83	Right_MinCutBalDivSum_FiberNDivLength	0.1280 0.1202	0.00000	0.00060	0.11071
463	All_MinCutBalDivSum_FiberN	0.0247 0.0211	0.00000	0.00062	0.11205
129	Right_MinCutBalDivSum_Unweighted	0.1884 0.1761	0.00000	0.00062	0.11229
1015	Left_Sum_FiberN	6803.8333 6627.2168	0.00006	0.00068	0.12183
234	All_MinSpanningForest_FiberLengthMean	2800.7846 2827.1182	0.00013	0.00069	0.12438
463	Left_MinSpanningForest_FAMean	47.5061 45.7752	0.00000	0.00071	0.12586
83	Right_LogSpanningForestN_FiberN	189.8663 188.1787	0.00001	0.00072	0.12740
234	Left_MinSpanningForest_FAMean	25.2698 24.2600	0.00000	0.00072	0.12714
463	Left_Sum_FAMean	497.9572 473.8789	0.00000	0.00078	0.13569
1015	All_MinCutBalDivSum_FiberN	0.0240 0.0206	0.00000	0.00080	0.13954
1015	All_MinSpanningForest_FAMean	201.9819 195.954	0.00010	0.00088	0.15161
83	Left_HoffmanBound_Unweighted	4.7029 4.6025	0.00000	0.00092	0.15799
234	All_MinCutBalDivSum_FiberN	0.0255 0.0219	0.00001	0.00093	0.15874
83	All_HoffmanBound_Unweighted	4.5455 4.4635	0.00000	0.00095	0.16097
463	All_Sum_FiberNDivLength	652.6090 636.4074	0.00004	0.00098	0.16550
83	Left_AdjLMaxDivD_FiberN	1.9219 1.9959	0.00011	0.00099	0.16601
234	Right_HoffmanBound_FiberNDivLength	2.5444 2.492	0.00005	0.00100	0.16766
129	Left_MinVertexCover_FAMean	14.4665 14.0373	0.00000	0.00102	0.16859
463	Right_HoffmanBound_FiberNDivLength	2.4528 2.4067	0.00005	0.00113	0.18633
234	All_LogSpanningForestN_FAMean	326.5297 314.2237	0.00000	0.00118	0.19275
234	Right_PGEigengap_FAMean	0.1358 0.1245	0.00000	0.00123	0.20085
83	Left_HoffmanBound_FAMean	4.54790 4.4467	0.00004	0.00124	0.20121
83	Right_MinCutBalDivSum_FAMean	0.2459 0.2343	0.00000	0.00127	0.20401
1015	All_AdjLMaxDivD_Unweighted	2.8024 2.7315	0.00035	0.00133	0.21263
129	Right_PGEigengap_FiberLengthMean	0.2294 0.2076	0.00000	0.00137	0.21729
234	Left_LogSpanningForestN_FAMean	160.7687 153.7631	0.00000	0.00149	0.23541
234	Left_MinVertexCover_FAMean	25.5400 24.8354	0.00000	0.00155	0.24260
83	All_MinCutBalDivSum_FiberN	0.0301 0.0262	0.00004	0.00160	0.25006
129	All_MinCutBalDivSum_FiberN	0.0270 0.0234	0.00001	0.00172	0.26733
463	All_MinCutBalDivSum_FiberNDivLength	0.0247 0.0207	0.00009	0.00177	0.27216
83	Left_MaxMatching_FAMean	9.0821 8.8091	0.00000	0.00182	0.27878
1015	All_LogSpanningForestN_FiberNDivLength	-350.6301 -371.0974	0.00003	0.00183	0.27877
463	Right_Sum_FiberN	6464.768 6321.2048	0.00000	0.00187	0.28166
1015	Right_MinSpanningForest_FAMean	104.1024 100.8625	0.00063	0.00192	0.28781
463	Left_PGEigengap_FiberN	0.0639 0.0533	0.00077	0.00193	0.28752
129	Right_AdjLMaxDivD_Unweighted	1.2663 1.2554	0.00003	0.00200	0.29568
234	Right_MinCutBalDivSum_Unweighted	0.1346 0.1248	0.00000	0.00204	0.29922
129	Right_PGEigengap_FiberN	0.1213 0.1122	0.00000	0.00219	0.31972

1015	Right_HoffmanBound_FiberNDivLength	2.3635 2.3224	0.00001	0.00223	0.32298
129	Right_Sum_FiberNDivLength	260.6268 253.0514	0.00002	0.00224	0.32299
129	Left_LogSpanningForestN_Unweighted	160.6906 158.8977	0.00181	0.00230	0.32843
1015	All_Sum_FiberNDivLength	674.9224 659.8373	0.00051	0.00242	0.34341
234	Left_Sum_FiberNDivLength	307.8607 298.9560	0.00180	0.00251	0.35422
1015	Left_AdjLMaxDivD_FiberN	7.2625 7.6401	0.00670	0.00256	0.35855
1015	Left_LogSpanningForestN_FiberNDivLength	-172.7454 -184.1958	0.00045	0.00257	0.35757
1015	Right_Sum_FiberN	6558.825 6419.7951	0.00000	0.00260	0.35831
234	Right_MinCutBalDivSum_FiberLengthMean	0.14285 0.1300	0.00000	0.00261	0.35696
83	Right_Sum_Unweighted	258.9098 252.433	0.00000	0.00262	0.35612
463	Right_Sum_FAMean	511.0996 490.0837	0.00000	0.00263	0.35544
129	Left_MinSpanningForest_FAMean	14.6338 13.9911	0.00000	0.00288	0.38627
129	Right_HoffmanBound_FAMean	4.4157 4.3338	0.00169	0.00305	0.40579
129	All_LogSpanningForestN_Unweighted	320.12464 317.1016	0.00022	0.00307	0.40566
83	Left_MaxFracMatching_FAMean	9.1276 8.8673	0.00000	0.00311	0.40756
83	Left_MinVertexCover_FAMean	9.1276 8.8673	0.00000	0.00311	0.40444
129	Right_Sum_Unweighted	473.3083 461.3614	0.00000	0.00336	0.43345
234	Right_LogSpanningForestN_FAMean	161.2133 155.8611	0.00005	0.00417	0.53417
83	All_MaxMatching_FiberN	2409.5901 2350.9397	0.00065	0.00426	0.54130
1015	Right_MinVertexCover_Unweighted	209.0 212.1686	0.00018	0.00440	0.55470
1015	Right_MaxMatching_Unweighted	208.825 211.9036	0.00023	0.00441	0.55173
1015	Right_MaxFracMatching_Unweighted	209.0125 212.0963	0.00048	0.00467	0.57851
463	Left_AdjLMaxDivD_FiberN	3.9863 4.1652	0.00752	0.00472	0.58107
83	All_MaxFracMatching_FiberN	2413.9795 2353.6987	0.00018	0.00482	0.58813
83	All_MinVertexCover_FiberN	2413.9795 2353.6987	0.00018	0.00482	0.58330
463	Left_PGEigengap_Unweighted	0.0716 0.0609	0.00189	0.00502	0.60187
83	Left_MinSpanningForest_FAMean	9.6386 9.1950	0.00000	0.00509	0.60605
234	All_Sum_Unweighted	1799.575 1764.3373	0.00000	0.00521	0.61534
463	All_MinVertexCover_FAMean	88.9526 86.9509	0.00196	0.00538	0.62967
234	Right_PGEigengap_FiberLengthMean	0.1428 0.1302	0.00000	0.00539	0.62543
129	Right_LogSpanningForestN_FiberN	289.9664 288.0403	0.00013	0.00567	0.65178
83	Right_MinCutBalDivSum_FiberLengthMean	0.2340 0.2218	0.00000	0.00571	0.65079
1015	Left_MinSpanningForest_FAMean	98.0028 95.2974	0.00024	0.00659	0.74520
463	Left_PGEigengap_FAMean	0.0835 0.07132	0.00319	0.00661	0.74045
463	Right_HoffmanBound_FiberN	2.3990 2.36062	0.00045	0.00671	0.74462
234	Right_MinCutBalDivSum_FiberN	0.0956 0.0898	0.00000	0.00702	0.77239
1015	All_MaxFracMatching_Unweighted	418.3739 424.0783	0.00017	0.00781	0.85172
463	Left_PGEigengap_FiberNDivLength	0.0465 0.0403	0.00312	0.00822	0.88762
234	Left_Sum_Unweighted	908.525 889.7228	0.00012	0.00841	0.89999
463	Left_PGEigengap_FiberLengthMean	0.0880 0.07505	0.00663	0.00884	0.93695
1015	Right_MinVertexCoverBinary_Unweighted	228.4 232.75903	0.00179	0.00898	0.94273
129	Left_AdjLMaxDivD_FiberN	1.8683 1.9385	0.0006	0.00905	0.94119
1015	All_MinVertexCover_Unweighted	417.625 423.2222	0.00009	0.00924	0.95151
83	Left_Sum_FiberLengthMean	8672.8595 8232.6217	0.00946	0.00958	0.97707
83	Right_PGEigengap_FiberLengthMean	0.3343 0.3134	0.00000	0.01002	1.01235
463	Left_MinVertexCover_FAMean	43.4996 42.4814	0.00078	0.01018	1.01839
129	Right_MinCutBalDivSum_FiberN	0.1108 0.10464	0.00000	0.01064	1.05338
129	Left_HoffmanBound_Unweighted	4.7137 4.6438	0.00040	0.01072	1.05098
1015	All_Sum_FAMean	1444.4965 1398.4729	0.00001	0.01224	1.18762
463	Right_MinCutBalDivSum_Unweighted	0.0918 0.0861	0.00000	0.01227	1.17782
234	All_PGEigengap_FAMean	0.0190 0.0172	0.00376	0.01229	1.16788
83	Right_PGEigengap_FiberN	0.1696 0.1605	0.00000	0.01275	1.19877
1015	All_MinVertexCoverBinary_Unweighted	457.9416 465.8313	0.00021	0.01303	1.21160
129	All_PGEigengap_FAMean	0.0315 0.0288	0.00611	0.01317	1.21205
234	Right_HoffmanBound_FiberN	2.5314 2.4861	0.00274	0.01325	1.20545
83	All_Sum_FiberLengthMean	16888.8359 16180.3784	0.00227	0.01364	1.22751
129	Left_AdjLMaxDivD_FAMean	1.3767 1.3947	0.00366	0.01387	1.23455
1015	All_MaxFracMatching_FiberN	2489.2041 2447.0120	0.00000	0.01440	1.26697
463	Left_LogSpanningForestN_FAMean	211.7869 202.0911	0.00019	0.01528	1.32939
463	All_PGEigengap_FiberNDivLength	0.0177 0.0149	0.0029	0.01609	1.38336
1015	Left_AdjLMaxDivD_Unweighted	2.7123 2.6596	0.00095	0.01668	1.41741
463	All_AdjLMaxDivD_Unweighted	1.8766 1.8486	0.00023	0.01701	1.42876
1015	Left_Sum_FAMean	709.6940 685.9307	0.00003	0.01734	1.43905
234	Right_Sum_FiberNDivLength	292.9252 286.7967	0.00046	0.01734	1.42191
83	Right_AdjLMaxDivD_Unweighted	1.2546 1.2472	0.00357	0.01771	1.43452
1015	All_MaxMatching_FiberN	2486.8166 2446.6626	0.00000	0.01863	1.49000
83	Right_HoffmanBound_FiberNDivLength	2.6162 2.5597	0.00012	0.02098	1.65710
1015	All_LogSpanningForestN_FAMean	457.4291 429.4160	0.00002	0.02193	1.71079

463	Right_MinVertexCoverBinary_Unweighted	138.8842 140.6385	0.00346	0.02211	1.70228
463	Right_PGEigengap_FiberNDivLength	0.0510 0.0468	0.00011	0.02227	1.69242
463	All_LogSpanningForestN_FAMean	443.0184 426.4406	0.00033	0.02327	1.74559
83	All_HoffmanBound_FAMean	4.3274 4.2704	0.00000	0.02581	1.90979
234	All_PGEigengap_Unweighted	0.01750 0.0161	0.00442	0.02653	1.93685
1015	All_MinVertexCover_FiberN	2491.4166 2452.9036	0.00000	0.02842	2.04607
234	All_LogSpanningForestN_FiberN	955.4761 950.29269	0.00178	0.02972	2.11030
1015	Right_Sum_FAMean	723.2379 702.4680	0.00005	0.03022	2.11561
463	Right_MaxMatching_Unweighted	110.6859 111.2048	0.00204	0.03132	2.16131
1015	Right_LogSpanningForestN_FiberNDivLength	-183.9473 -192.2899	0.00128	0.03399	2.31135
1015	All_MinCutBalDivSum_Unweighted	0.0066 0.00160	0.00518	0.03489	2.33738
1015	Left_LogSpanningForestN_FAMean	217.4574 203.1308	0.00005	0.03649	2.40862
129	Right_LogSpanningForestN_Unweighted	153.7504 152.5235	0.00329	0.03858	2.50795
1015	Right_LogSpanningForestN_FAMean	233.3453 219.9728	0.00017	0.03912	2.50390
234	Right_Sum_Unweighted	866.725 852.1807	0.00005	0.04054	2.55409
463	Right_PGEigengap_Unweighted	0.0705 0.0649	0.00008	0.04133	2.56240
129	All_PGEigengap_Unweighted	0.0299 0.0279	0.00644	0.04404	2.68649
463	Right_MinCutBalDivSum_FiberLengthMean	0.0956 0.0896	0.00000	0.04584	2.75064
463	All_MaxFracMatching_Unweighted	222.3057 223.2168	0.00011	0.04727	2.78883
463	All_MaxMatching_Unweighted	222.1735 223.0120	0.00006	0.05127	2.97341
83	All_MaxFracMatching_FiberNDivLength	109.988 107.7572	0.00221	0.05169	2.94617
83	All_MinVertexCover_FiberNDivLength	109.9887 107.7572	0.00221	0.05169	2.89448
463	All_MinVertexCover_Unweighted	222.3388 223.2289	0.00010	0.05250	2.88729
463	Right_Sum_FiberNDivLength	311.3203 306.3797	0.00331	0.05424	2.92881
463	Right_PGEigengap_FiberN	0.0661 0.0611	0.00009	0.05453	2.89026
463	Right_MinVertexCover_Unweighted	110.9380 111.4216	0.00259	0.05539	2.88018
1015	Left_MinVertexCoverBinary_Unweighted	229.2583 232.6746	0.00034	0.05953	3.03594
1015	Left_MaxFracMatching_Unweighted	209.3666 211.7048	0.00118	0.06019	3.00930
463	Right_MaxFracMatching_Unweighted	110.9256 111.3855	0.00309	0.06695	3.28031
129	All_Sum_FiberLengthMean	30088.0733 29148.1015	0.00412	0.07048	3.38324
83	Right_LogSpanningForestN_Unweighted	89.7645 89.0820	0.00089	0.07272	3.41764
1015	Left_MinVertexCover_Unweighted	209.1916 211.4337	0.00104	0.07578	3.48604
1015	Right_MinSpanningForest_FiberN	473.825 477.9277	0.00337	0.07800	3.51010
463	All_MinVertexCoverBinary_Unweighted	277.2396 279.67469	0.00020	0.07991	3.51606
129	All_HoffmanBound_FAMean	4.3668 4.3276	0.00372	0.08437	3.62771
234	Right_MinSpanningForest_FiberLengthMean	1370.9407 1378.45522	0.00707	0.08438	3.54390
463	All_MinSpanningForest_FiberLengthMean	5356.4309 5385.0509	0.00627	0.08536	3.49962
83	Right_HoffmanBound_Unweighted	4.6113 4.5608	0.00006	0.08584	3.43357
463	Right_LogSpanningForestN_FAMean	225.9686 219.2312	0.00395	0.08786	3.42655
463	Right_PGEigengap_FAMean	0.0826 0.0771	0.00007	0.08842	3.35998
1015	Left_MaxMatching_Unweighted	209.2833 211.36143	0.00055	0.08938	3.30714
83	All_MaxMatching_FiberNDivLength	109.5831 107.6791	0.00650	0.09423	3.39233
83	Right_MinCutBalDivSum_FiberN	0.1287 0.12476	0.00000	0.09707	3.39755
129	Right_Sum_FiberLengthMean	13908.4549 13470.3465	0.00837	0.10380	3.52934
83	Right_HoffmanBound_FAMean	4.4308 4.3780	0.00000	0.10389	3.42821
83	Right_Sum_FiberLengthMean	7631.6042 7392.1456	0.00300	0.11548	3.69535
463	Left_MaxFracMatching_Unweighted	111.3760 111.8072	0.00022	0.13062	4.04908
463	Right_PGEigengap_FiberLengthMean	0.0857 0.08013	0.00052	0.13259	3.97768
463	All_AdjLMaxDivD_FiberNDivLength	5.0105 4.8826	0.00063	0.14493	4.20303
234	All_Sum_FiberLengthMean	50705.6991 49509.7827	0.00472	0.14614	4.09197
1015	All_MinSpanningForest_FiberN	951.7333 956.9518	0.00215	0.14956	4.03800
129	All_AdjLMaxDivD_Unweighted	1.3009 1.2950	0.00391	0.15217	3.95652
463	All_MaxMatching_FiberN	2408.5619 2385.506	0.00003	0.16612	4.15299
234	Left_Sum_FiberLengthMean	25968.3400 25333.5608	0.00808	0.16909	4.05805
463	Left_MinSpanningForest_FiberLengthMean	2693.9037 2708.0471	0.00029	0.16935	3.89511
463	Left_MinVertexCover_Unweighted	111.3966 111.7831	0.00020	0.17471	3.84373
463	Right_MinCutBalDivSum_FiberN	0.0720 0.0698	0.00000	0.18380	3.85985
1015	Right_MinCutBalDivSum_Unweighted	0.0567 0.0548	0.00000	0.20002	4.00031
463	All_MinVertexCover_FiberN	2414.3842 2392.3313	0.00003	0.20040	3.80760
463	Left_AdjLMaxDivD_Unweighted	1.8456 1.8312	0.00037	0.21019	3.78341
463	All_MaxFracMatching_FiberN	2414.38429 2393.3915	0.00004	0.22266	3.78530
1015	All_AdjLMaxDivD_FiberNDivLength	9.8369 9.6047	0.00022	0.23128	3.70054
234	All_AdjLMaxDivD_FiberNDivLength	2.9784 2.9251	0.00578	0.23787	3.56812
234	Right_LogSpanningForestN_FiberN	464.4918 462.8764	0.00579	0.23915	3.34810
1015	Right_MinSpanningForest_FiberNDivLength	21.3594 21.58465	0.00392	0.33018	4.29233
463	Left_MaxMatching_Unweighted	111.2975 111.5662	0.00011	0.33520	4.02238
234	All_MaxMatching_FiberN	2403.8 2387.5180	0.00037	0.33724	3.70960
129	All_MaxFracMatching_FiberN	2418.9208 2403.0180	0.00167	0.34902	3.49021

1015	Right_MinCutBalDivSum_FiberLengthMean	0.0577 0.0559	0.00006	0.35609	3.20477
129	All_MaxMatching_FiberN	2412.5 2396.9156	0.00155	0.36285	2.90276
463	Left_MinVertexCoverBinary_Unweighted	138.0165 138.6987	0.00028	0.37344	2.61406
129	All_MinVertexCover_FiberN	2415.5041 2401.6325	0.00145	0.43115	2.58690
1015	Right_MinCutBalDivSum_FiberN	0.0470 0.0462	0.00001	0.45084	2.25419
234	All_MinVertexCover_FiberN	2411.820 2399.3012	0.00010	0.46896	1.87582
234	All_MaxFracMatching_FiberN	2409.7791 2398.1445	0.00032	0.49808	1.49424
129	Left_AdjLMaxDivD_Unweighted	1.2641 1.2625	0.00166	0.62457	1.24914
1015	All_MinSpanningForest_FiberNDivLength	42.7199 42.8768	0.00901	0.66464	0.66464

7.2. Table 2

Table 2: In this table, we give the graph-theoretic parameters computed for the 83-vertex graphs. The table contains their arithmetic means in the male and female groups, and the corresponding p-values for group 0 (see the “Statistical analysis” subsection). The graph-parameters and the syntax of the data are defined in the main text. Significant differences ($p < 0.01$) are denoted with an asterisk in the last column.

Property	Female	Male	p-value	
All_AdjLMaxDivD_FAMean	1.36875	1.38259	0.01187	
All_AdjLMaxDivD_FiberLengthMean	1.44867	1.44343	0.54869	
All_AdjLMaxDivD_FiberN	2.05880	2.11497	0.01035	
All_AdjLMaxDivD_FiberNDivLength	1.86494	1.86145	0.80141	
All_AdjLMaxDivD_Unweighted	1.26969	1.26372	0.07134	
All_HoffmanBound_FAMean	4.33196	4.19675	0.00000	*
All_HoffmanBound_FiberLengthMean	3.22244	3.18444	0.15967	
All_HoffmanBound_FiberN	2.62571	2.59760	0.14184	
All_HoffmanBound_FiberNDivLength	2.50583	2.46965	0.06702	
All_HoffmanBound_Unweighted	4.54119	4.39769	0.00000	*
All_LeftRatio_FAMean	0.96407	0.96324	0.87951	
All_LeftRatio_FiberLengthMean	1.01790	1.02383	0.40343	
All_LeftRatio_FiberN	0.98798	0.99695	0.09018	
All_LeftRatio_FiberNDivLength	0.98714	0.99320	0.21746	
All_LeftRatio_Unweighted	0.99363	0.99763	0.29970	
All_LogSpanningForestN_FAMean	108.57625	99.82325	0.00000	*
All_LogSpanningForestN_FiberLengthMean	454.30207	452.11354	0.15516	
All_LogSpanningForestN_FiberN	395.98463	391.08233	0.00000	*
All_LogSpanningForestN_FiberNDivLength	147.77314	142.42711	0.00000	*
All_LogSpanningForestN_Unweighted	190.48531	187.73945	0.00004	*
All_MaxFracMatching_FAMean	18.46840	17.58077	0.00000	*
All_MaxFracMatching_FiberLengthMean	2009.76723	1975.53559	0.34678	
All_MaxFracMatching_FiberN	2426.47391	2344.52660	0.00018	*
All_MaxFracMatching_FiberNDivLength	111.31000	107.40786	0.00221	*
All_MaxFracMatching_Unweighted	40.80000	40.94681	0.01166	
All_MaxMatching_FAMean	18.44825	17.52991	0.00000	*
All_MaxMatching_FiberLengthMean	2008.89813	1979.58130	0.41489	
All_MaxMatching_FiberN	2418.51304	2346.44681	0.00065	*
All_MaxMatching_FiberNDivLength	110.89315	107.45589	0.00650	*
All_MaxMatching_Unweighted	40.53043	40.67021	0.04499	
All_MinCutBalDivSum_FAMean	0.04102	0.03885	0.12673	
All_MinCutBalDivSum_FiberLengthMean	0.03239	0.03182	0.74907	

All_MinCutBalDivSum_FiberN	0.02940	0.02436	0.00004	*
All_MinCutBalDivSum_FiberNDivLength	0.03340	0.02661	0.00000	*
All_MinCutBalDivSum_Unweighted	0.04008	0.03789	0.11561	
All_MinSpanningForest_FAMean	19.67830	18.19979	0.00000	*
All_MinSpanningForest_FiberLengthMean	1093.76872	1112.08242	0.00017	*
All_MinSpanningForest_FiberN	101.08696	103.47872	0.03254	
All_MinSpanningForest_FiberNDivLength	3.64724	3.70903	0.45315	
All_MinVertexCoverBinary_Unweighted	59.19130	59.07447	0.52716	
All_MinVertexCover_FAMean	18.46840	17.58077	0.00000	*
All_MinVertexCover_FiberLengthMean	2009.76723	1975.53559	0.34678	
All_MinVertexCover_FiberN	2426.47391	2344.52660	0.00018	*
All_MinVertexCover_FiberNDivLength	111.31000	107.40786	0.00221	*
All_MinVertexCover_Unweighted	40.80000	40.94681	0.01166	
All_PGEigengap_FAMean	0.05398	0.05032	0.03291	
All_PGEigengap_FiberLengthMean	0.04269	0.04155	0.58068	
All_PGEigengap_FiberN	0.03111	0.02622	0.00000	*
All_PGEigengap_FiberNDivLength	0.03400	0.02787	0.00000	*
All_PGEigengap_Unweighted	0.05187	0.04818	0.01977	
All_Sum_FAMean	217.42826	195.09313	0.00000	*
All_Sum_FiberLengthMean	16574.03831	15653.05783	0.00227	*
All_Sum_FiberN	11129.93913	10353.87234	0.00000	*
All_Sum_FiberNDivLength	475.82094	445.36396	0.00000	*
All_Sum_Unweighted	560.69565	537.21277	0.00000	*
Left_AdjLMaxDivD_FAMean	1.33861	1.35695	0.00276	*
Left_AdjLMaxDivD_FiberLengthMean	1.39587	1.38727	0.25905	
Left_AdjLMaxDivD_FiberN	1.93777	2.02636	0.00011	*
Left_AdjLMaxDivD_FiberNDivLength	1.73693	1.77462	0.01256	
Left_AdjLMaxDivD_Unweighted	1.24166	1.23423	0.02696	
Left_HoffmanBound_FAMean	4.53589	4.39998	0.00004	*
Left_HoffmanBound_FiberLengthMean	3.26475	3.21357	0.09120	
Left_HoffmanBound_FiberN	2.71677	2.69771	0.41879	
Left_HoffmanBound_FiberNDivLength	2.65881	2.61979	0.16775	
Left_HoffmanBound_Unweighted	4.69319	4.53245	0.00000	*
Left_LogSpanningForestN_FAMean	52.60202	47.79692	0.00000	*
Left_LogSpanningForestN_FiberLengthMean	228.00986	227.07923	0.30936	
Left_LogSpanningForestN_FiberN	198.46664	196.34346	0.00045	*
Left_LogSpanningForestN_FiberNDivLength	73.79704	71.25881	0.00001	*
Left_LogSpanningForestN_Unweighted	94.79835	93.39721	0.00117	*
Left_MaxFracMatching_FAMean	9.13784	8.64312	0.00000	*
Left_MaxFracMatching_FiberLengthMean	1055.51350	1041.51094	0.50266	
Left_MaxFracMatching_FiberN	1168.49565	1155.44681	0.33894	
Left_MaxFracMatching_FiberNDivLength	54.85027	53.06283	0.01912	
Left_MaxFracMatching_Unweighted	20.70870	20.78723	0.03546	
Left_MaxMatching_FAMean	9.11166	8.60492	0.00000	*
Left_MaxMatching_FiberLengthMean	1052.74695	1046.89693	0.77946	
Left_MaxMatching_FiberN	1165.86087	1157.89362	0.54454	
Left_MaxMatching_FiberNDivLength	54.71769	53.09956	0.02948	
Left_MaxMatching_Unweighted	20.44348	20.59574	0.02850	
Left_MinCutBalDivSum_FAMean	0.24446	0.22566	0.00001	*
Left_MinCutBalDivSum_FiberLengthMean	0.23339	0.21318	0.00003	*

Left_MinCutBalDivSum_FiberN	0.12873	0.11341	0.00000	*
Left_MinCutBalDivSum_FiberNDivLength	0.13168	0.11676	0.00000	*
Left_MinCutBalDivSum_Unweighted	0.24046	0.22316	0.00000	*
Left_MinSpanningForest_FAMean	9.64023	8.84224	0.00000	*
Left_MinSpanningForest_FiberLengthMean	555.69180	565.67296	0.00146	*
Left_MinSpanningForest_FiberN	52.26087	54.69149	0.02852	
Left_MinSpanningForest_FiberNDivLength	1.85125	1.95886	0.15079	
Left_MinVertexCoverBinary_Unweighted	29.99130	29.89362	0.50013	
Left_MinVertexCover_FAMean	9.13784	8.64312	0.00000	*
Left_MinVertexCover_FiberLengthMean	1055.51350	1041.51094	0.50266	
Left_MinVertexCover_FiberN	1168.49565	1155.44681	0.33894	
Left_MinVertexCover_FiberNDivLength	54.85027	53.06283	0.01912	
Left_MinVertexCover_Unweighted	20.70870	20.78723	0.03546	
Left_PGEigengap_FAMean	0.32901	0.29424	0.00000	*
Left_PGEigengap_FiberLengthMean	0.32651	0.29063	0.00000	*
Left_PGEigengap_FiberN	0.16362	0.14119	0.00000	*
Left_PGEigengap_FiberNDivLength	0.13964	0.12469	0.00000	*
Left_PGEigengap_Unweighted	0.30169	0.26858	0.00000	*
Left_Sum_FAMean	104.90524	93.93956	0.00000	*
Left_Sum_FiberLengthMean	8454.81314	8010.01349	0.00946	*
Left_Sum_FiberN	5496.91304	5155.82979	0.00000	*
Left_Sum_FiberNDivLength	234.67696	221.00148	0.00000	*
Left_Sum_Unweighted	278.78261	267.84043	0.00000	*
Right_AdjLMaxDivD_FAMean	1.34243	1.34454	0.71444	
Right_AdjLMaxDivD_FiberLengthMean	1.41086	1.41093	0.99277	
Right_AdjLMaxDivD_FiberN	2.05169	2.10053	0.03725	
Right_AdjLMaxDivD_FiberNDivLength	1.79625	1.79740	0.93925	
Right_AdjLMaxDivD_Unweighted	1.25612	1.24659	0.00357	*
Right_HoffmanBound_FAMean	4.46780	4.30965	0.00000	*
Right_HoffmanBound_FiberLengthMean	3.34214	3.31686	0.41097	
Right_HoffmanBound_FiberN	2.64848	2.59375	0.01381	
Right_HoffmanBound_FiberNDivLength	2.62271	2.52700	0.00012	*
Right_HoffmanBound_Unweighted	4.61029	4.48940	0.00006	*
Right_LogSpanningForestN_FAMean	50.77679	47.15788	0.00000	*
Right_LogSpanningForestN_FiberLengthMean	217.22296	216.02568	0.17484	
Right_LogSpanningForestN_FiberN	189.95076	187.56201	0.00001	*
Right_LogSpanningForestN_FiberNDivLength	69.45578	67.16406	0.00000	*
Right_LogSpanningForestN_Unweighted	89.59331	88.39743	0.00089	*
Right_MaxFracMatching_FAMean	9.15030	8.78620	0.00004	*
Right_MaxFracMatching_FiberLengthMean	934.52521	912.03714	0.22786	
Right_MaxFracMatching_FiberN	1169.82174	1154.66489	0.25487	
Right_MaxFracMatching_FiberNDivLength	54.37426	53.80631	0.44887	
Right_MaxFracMatching_Unweighted	20.09130	20.17021	0.10789	
Right_MaxMatching_FAMean	9.12190	8.74960	0.00003	*
Right_MaxMatching_FiberLengthMean	935.16155	909.69912	0.16516	
Right_MaxMatching_FiberN	1167.60870	1154.00000	0.29447	
Right_MaxMatching_FiberNDivLength	54.16573	53.82448	0.64463	
Right_MaxMatching_Unweighted	19.83478	19.89362	0.22290	
Right_MinCutBalDivSum_FAMean	0.24426	0.22199	0.00000	*
Right_MinCutBalDivSum_FiberLengthMean	0.23356	0.21038	0.00000	*

Right_MinCutBalDivSum_FiberN	0.13295	0.11836	0.00000	*
Right_MinCutBalDivSum_FiberNDivLength	0.12923	0.11715	0.00000	*
Right_MinCutBalDivSum_Unweighted	0.23636	0.21557	0.00000	*
Right_MinSpanningForest_FAMean	10.18720	9.53901	0.00019	*
Right_MinSpanningForest_FiberLengthMean	535.98644	542.59066	0.02855	
Right_MinSpanningForest_FiberN	51.97391	52.17021	0.80170	
Right_MinSpanningForest_FiberNDivLength	1.95546	1.95190	0.94388	
Right_MinVertexCoverBinary_Unweighted	28.72174	28.82979	0.38707	
Right_MinVertexCover_FAMean	9.15030	8.78620	0.00004	*
Right_MinVertexCover_FiberLengthMean	934.52521	912.03714	0.22786	
Right_MinVertexCover_FiberN	1169.82174	1154.66489	0.25487	
Right_MinVertexCover_FiberNDivLength	54.37426	53.80631	0.44887	
Right_MinVertexCover_Unweighted	20.09130	20.17021	0.10789	
Right_PGEigengap_FAMean	0.32003	0.28361	0.00000	*
Right_PGEigengap_FiberLengthMean	0.32906	0.28911	0.00000	*
Right_PGEigengap_FiberN	0.17370	0.15054	0.00000	*
Right_PGEigengap_FiberNDivLength	0.14931	0.13170	0.00000	*
Right_PGEigengap_Unweighted	0.29208	0.25911	0.00000	*
Right_Sum_FAMean	102.93685	92.99858	0.00000	*
Right_Sum_FiberLengthMean	7545.43741	7105.85395	0.00300	*
Right_Sum_FiberN	5297.13913	4936.30851	0.00000	*
Right_Sum_FiberNDivLength	224.73904	212.15506	0.00000	*
Right_Sum_Unweighted	258.13043	247.79787	0.00000	*

7.3. Table 3

Table 3: In this table, we give the graph-theoretic parameters computed for the 129-vertex graphs. The table contains their arithmetic means in the male and female groups, and the corresponding p-values for group 0 (see the “Statistical analysis” subsection). The graph-parameters and the syntax of the data are defined in the main text. Significant differences ($p < 0.01$) are denoted with an asterisk in the last column.

Property	Female	Male	p-value	
All_AdjLMaxDivD_FAMean	1.41064	1.42178	0.08520	
All_AdjLMaxDivD_FiberLengthMean	1.49498	1.49885	0.68478	
All_AdjLMaxDivD_FiberN	2.18019	2.21788	0.12879	
All_AdjLMaxDivD_FiberNDivLength	2.09142	2.04274	0.02144	
All_AdjLMaxDivD_Unweighted	1.30068	1.28949	0.00391	*
All_HoffmanBound_FAMean	4.37021	4.30605	0.00372	*
All_HoffmanBound_FiberLengthMean	3.23335	3.22805	0.84136	
All_HoffmanBound_FiberN	2.50847	2.50227	0.73403	
All_HoffmanBound_FiberNDivLength	2.38060	2.42236	0.04465	
All_HoffmanBound_Unweighted	4.59120	4.49569	0.00004	*
All_LeftRatio_FAMean	0.99194	0.99322	0.80077	
All_LeftRatio_FiberLengthMean	1.03504	1.03831	0.59672	
All_LeftRatio_FiberN	0.98611	0.99449	0.08462	
All_LeftRatio_FiberNDivLength	0.98580	0.99159	0.20592	
All_LeftRatio_Unweighted	1.01296	1.01593	0.37175	
All_LogSpanningForestN_FAMean	190.78404	178.44384	0.00000	*

All_LogSpanningForestN_FiberLengthMean	734.96618	731.41772	0.13256	
All_LogSpanningForestN_FiberN	597.06042	591.32147	0.00000	*
All_LogSpanningForestN_FiberNDivLength	210.12907	204.62471	0.00000	*
All_LogSpanningForestN_Unweighted	319.83789	316.08121	0.00022	*
All_MaxFracMatching_FAMean	49.65353	50.66528	0.66683	
All_MaxFracMatching_FiberLengthMean	3200.56758	3155.33612	0.40310	
All_MaxFracMatching_FiberN	2439.32018	2379.91489	0.00167	*
All_MaxFracMatching_FiberNDivLength	129.54868	128.84984	0.66147	
All_MaxFracMatching_Unweighted	63.77193	63.92021	0.01429	
All_MaxMatching_FAMean	49.46172	50.45366	0.67164	
All_MaxMatching_FiberLengthMean	3195.95938	3150.79561	0.40248	
All_MaxMatching_FiberN	2433.70175	2373.79787	0.00155	*
All_MaxMatching_FiberNDivLength	129.14480	128.43086	0.65416	
All_MaxMatching_Unweighted	63.51754	63.63830	0.09249	
All_MinCutBalDivSum_FAMean	0.04566	0.04964	0.19728	
All_MinCutBalDivSum_FiberLengthMean	0.01816	0.01776	0.69091	
All_MinCutBalDivSum_FiberN	0.02662	0.02160	0.00001	*
All_MinCutBalDivSum_FiberNDivLength	0.04857	0.04496	0.15218	
All_MinCutBalDivSum_Unweighted	0.02263	0.02118	0.06676	
All_MinSpanningForest_FAMean	29.88114	27.89533	0.00000	*
All_MinSpanningForest_FiberLengthMean	1638.10279	1661.92149	0.00007	*
All_MinSpanningForest_FiberN	140.42105	141.07447	0.38283	
All_MinSpanningForest_FiberNDivLength	4.49632	4.44670	0.56203	
All_MinVertexCoverBinary_Unweighted	95.98246	95.95745	0.90908	
All_MinVertexCover_FAMean	29.21538	27.95197	0.00000	*
All_MinVertexCover_FiberLengthMean	3199.42585	3154.86947	0.40926	
All_MinVertexCover_FiberN	2440.16228	2379.91489	0.00145	*
All_MinVertexCover_FiberNDivLength	121.15928	119.62335	0.21405	
All_MinVertexCover_Unweighted	63.76754	63.92021	0.01118	
All_PGEigengap_FAMean	0.03177	0.02898	0.00611	*
All_PGEigengap_FiberLengthMean	0.02543	0.02424	0.33973	
All_PGEigengap_FiberN	0.02737	0.02259	0.00000	*
All_PGEigengap_FiberNDivLength	0.02816	0.02267	0.00000	*
All_PGEigengap_Unweighted	0.03039	0.02780	0.00644	*
All_Sum_FAMean	388.40124	352.11586	0.00000	*
All_Sum_FiberLengthMean	29828.05826	28284.32274	0.00412	*
All_Sum_FiberN	12257.67544	11610.31915	0.00000	*
All_Sum_FiberNDivLength	549.08397	524.10766	0.00000	*
All_Sum_Unweighted	1006.11404	966.30851	0.00000	*
Left_AdjLMaxDivD_FAMean	1.38198	1.40166	0.00366	*
Left_AdjLMaxDivD_FiberLengthMean	1.42577	1.42392	0.81274	
Left_AdjLMaxDivD_FiberN	1.87505	1.96425	0.00064	*
Left_AdjLMaxDivD_FiberNDivLength	1.78286	1.82451	0.03311	
Left_AdjLMaxDivD_Unweighted	1.26570	1.25571	0.00166	*
Left_HoffmanBound_FAMean	4.54921	4.48547	0.03131	
Left_HoffmanBound_FiberLengthMean	3.27052	3.26083	0.73075	
Left_HoffmanBound_FiberN	2.75397	2.75802	0.85517	
Left_HoffmanBound_FiberNDivLength	2.66995	2.66242	0.73338	
Left_HoffmanBound_Unweighted	4.73359	4.63754	0.00040	*
Left_LogSpanningForestN_FAMean	94.49928	87.83720	0.00000	*

Left_LogSpanningForestN_FiberLengthMean	369.71301	368.14978	0.22674	
Left_LogSpanningForestN_FiberN	299.76741	297.25592	0.00100	*
Left_LogSpanningForestN_FiberNDivLength	105.37888	102.73539	0.00023	*
Left_LogSpanningForestN_Unweighted	160.53197	158.68211	0.00181	*
Left_MaxFracMatching_FAMean	24.76152	25.29477	0.66522	
Left_MaxFracMatching_FiberLengthMean	1663.09920	1643.90725	0.52787	
Left_MaxFracMatching_FiberN	1167.39912	1152.96809	0.23422	
Left_MaxFracMatching_FiberNDivLength	63.38229	62.99647	0.67411	
Left_MaxFracMatching_Unweighted	32.19298	32.26064	0.07928	
Left_MaxMatching_FAMean	24.57217	25.09906	0.66544	
Left_MaxMatching_FiberLengthMean	1660.02044	1641.59413	0.54314	
Left_MaxMatching_FiberN	1164.21053	1150.29787	0.25202	
Left_MaxMatching_FiberNDivLength	63.13867	62.73563	0.65871	
Left_MaxMatching_Unweighted	31.97368	31.96809	0.81135	
Left_MinCutBalDivSum_FAMean	0.39150	0.41499	0.30927	
Left_MinCutBalDivSum_FiberLengthMean	0.19430	0.17341	0.00001	*
Left_MinCutBalDivSum_FiberN	0.12108	0.10120	0.00000	*
Left_MinCutBalDivSum_FiberNDivLength	0.29168	0.29222	0.97721	
Left_MinCutBalDivSum_Unweighted	0.19064	0.17241	0.00000	*
Left_MinSpanningForest_FAMean	14.54348	13.51233	0.00000	*
Left_MinSpanningForest_FiberLengthMean	824.76247	838.66139	0.00016	*
Left_MinSpanningForest_FiberN	71.20175	72.77660	0.11052	
Left_MinSpanningForest_FiberNDivLength	2.27718	2.29001	0.85866	
Left_MinVertexCoverBinary_Unweighted	48.64035	48.59574	0.77023	
Left_MinVertexCover_FAMean	14.51869	13.77702	0.00000	*
Left_MinVertexCover_FiberLengthMean	1663.75423	1643.77929	0.51100	
Left_MinVertexCover_FiberN	1167.29825	1152.96809	0.23644	
Left_MinVertexCover_FiberNDivLength	59.17693	58.52190	0.38417	
Left_MinVertexCover_Unweighted	32.18860	32.26064	0.06131	
Left_PGEigengap_FAMean	0.22060	0.19382	0.00000	*
Left_PGEigengap_FiberLengthMean	0.22653	0.19611	0.00001	*
Left_PGEigengap_FiberN	0.11793	0.09781	0.00000	*
Left_PGEigengap_FiberNDivLength	0.09286	0.07972	0.00000	*
Left_PGEigengap_Unweighted	0.19796	0.17162	0.00000	*
Left_Sum_FAMean	192.60222	174.73153	0.00000	*
Left_Sum_FiberLengthMean	15444.91099	14683.45752	0.01028	
Left_Sum_FiberN	6041.00877	5772.81915	0.00000	*
Left_Sum_FiberNDivLength	270.61012	259.95554	0.00014	*
Left_Sum_Unweighted	509.72807	490.96809	0.00000	*
Right_AdjLMaxDivD_FAMean	1.37358	1.37371	0.98425	
Right_AdjLMaxDivD_FiberLengthMean	1.43491	1.44388	0.32229	
Right_AdjLMaxDivD_FiberN	2.13247	2.19242	0.04382	
Right_AdjLMaxDivD_FiberNDivLength	1.86174	1.85384	0.68280	
Right_AdjLMaxDivD_Unweighted	1.26948	1.25386	0.00003	*
Right_HoffmanBound_FAMean	4.42153	4.33327	0.00169	*
Right_HoffmanBound_FiberLengthMean	3.32244	3.31805	0.87546	
Right_HoffmanBound_FiberN	2.65165	2.56198	0.00010	*
Right_HoffmanBound_FiberNDivLength	2.66235	2.60715	0.00255	*
Right_HoffmanBound_Unweighted	4.61996	4.50591	0.00001	*
Right_LogSpanningForestN_FAMean	91.35003	85.96894	0.00000	*

Right_LogSpanningForestN_FiberLengthMean	356.43808	354.61854	0.17398	
Right_LogSpanningForestN_FiberN	289.75572	286.91867	0.00013	*
Right_LogSpanningForestN_FiberNDivLength	100.25279	97.89746	0.00009	*
Right_LogSpanningForestN_Unweighted	153.49975	151.79142	0.00329	*
Right_MaxFracMatching_FAMean	24.77565	25.22270	0.69622	
Right_MaxFracMatching_FiberLengthMean	1520.51801	1494.98889	0.35418	
Right_MaxFracMatching_FiberN	1186.44298	1192.61170	0.62145	
Right_MaxFracMatching_FiberNDivLength	64.15821	65.33536	0.19327	
Right_MaxFracMatching_Unweighted	31.58333	31.66489	0.10839	
Right_MaxMatching_FAMean	24.59989	25.05318	0.68852	
Right_MaxMatching_FiberLengthMean	1517.57112	1492.71983	0.36588	
Right_MaxMatching_FiberN	1184.06140	1188.95745	0.69571	
Right_MaxMatching_FiberNDivLength	63.89435	64.98231	0.22657	
Right_MaxMatching_Unweighted	31.33333	31.44681	0.11506	
Right_MinCutBalDivSum_FAMean	0.37589	0.38949	0.51341	
Right_MinCutBalDivSum_FiberLengthMean	0.19107	0.16602	0.00000	*
Right_MinCutBalDivSum_FiberN	0.11322	0.09749	0.00000	*
Right_MinCutBalDivSum_FiberNDivLength	0.27941	0.27422	0.76733	
Right_MinCutBalDivSum_Unweighted	0.18819	0.16752	0.00000	*
Right_MinSpanningForest_FAMean	15.44134	14.52785	0.00009	*
Right_MinSpanningForest_FiberLengthMean	809.70438	818.75455	0.01354	
Right_MinSpanningForest_FiberN	70.29825	69.92553	0.47065	
Right_MinSpanningForest_FiberNDivLength	2.33507	2.28667	0.32437	
Right_MinVertexCoverBinary_Unweighted	46.94737	47.04255	0.54948	
Right_MinVertexCover_FAMean	14.53416	14.02524	0.00009	*
Right_MinVertexCover_FiberLengthMean	1518.88778	1494.74150	0.38002	
Right_MinVertexCover_FiberN	1186.40351	1192.61170	0.62123	
Right_MinVertexCover_FiberNDivLength	59.96806	60.58959	0.42947	
Right_MinVertexCover_Unweighted	31.58333	31.66489	0.10839	
Right_PGEigengap_FAMean	0.22308	0.19156	0.00000	*
Right_PGEigengap_FiberLengthMean	0.22862	0.19449	0.00000	*
Right_PGEigengap_FiberN	0.12475	0.10411	0.00000	*
Right_PGEigengap_FiberNDivLength	0.10095	0.08711	0.00000	*
Right_PGEigengap_Unweighted	0.20057	0.17212	0.00000	*
Right_Sum_FAMean	186.05021	169.14759	0.00000	*
Right_Sum_FiberLengthMean	13793.60649	13074.49495	0.00837	*
Right_Sum_FiberN	5876.42105	5578.19149	0.00000	*
Right_Sum_FiberNDivLength	262.24767	252.08253	0.00002	*
Right_Sum_Unweighted	472.35965	454.00000	0.00000	*

7.4. Table 4

Table 4: In this table, we give the graph-theoretic parameters computed for the 234-vertex graphs. The table contains their arithmetic means in the male and female groups, and the corresponding p-values for group 0 (see the “Statistical analysis” subsection). The graph-parameters and the syntax of the data are defined in the main text. Significant differences ($p < 0.01$) are denoted with an asterisk in the last column.

Property	Female	Male	p-value
----------	--------	------	---------

All_AdjLMaxDivD_FAMean	1.60508	1.61546	0.23293	
All_AdjLMaxDivD_FiberLengthMean	1.72307	1.73537	0.35606	
All_AdjLMaxDivD_FiberN	3.03189	3.02754	0.90851	
All_AdjLMaxDivD_FiberNDivLength	3.02286	2.90195	0.00578	*
All_AdjLMaxDivD_Unweighted	1.44658	1.43449	0.03742	
All_HoffmanBound_FAMean	4.06651	4.07749	0.59508	
All_HoffmanBound_FiberLengthMean	3.10629	3.14528	0.12360	
All_HoffmanBound_FiberN	2.34706	2.37219	0.13150	
All_HoffmanBound_FiberNDivLength	2.27630	2.30274	0.10670	
All_HoffmanBound_Unweighted	4.23289	4.21785	0.45061	
All_LeftRatio_FAMean	0.98930	0.98854	0.87192	
All_LeftRatio_FiberLengthMean	1.02634	1.02701	0.91245	
All_LeftRatio_FiberN	0.99363	1.00228	0.06766	
All_LeftRatio_FiberNDivLength	0.99635	1.00247	0.17117	
All_LeftRatio_Unweighted	1.01073	1.01336	0.46683	
All_LogSpanningForestN_FAMean	325.93700	306.72147	0.00000	*
All_LogSpanningForestN_FiberLengthMean	1310.63404	1303.74187	0.10907	
All_LogSpanningForestN_FiberN	953.27020	946.29487	0.00178	*
All_LogSpanningForestN_FiberNDivLength	260.96946	255.95413	0.00295	*
All_LogSpanningForestN_Unweighted	570.62920	565.61983	0.01393	
All_MaxFracMatching_FAMean	80.76738	82.78486	0.65868	
All_MaxFracMatching_FiberLengthMean	5173.35435	5071.70659	0.22429	
All_MaxFracMatching_FiberN	2421.71739	2361.18617	0.00032	*
All_MaxFracMatching_FiberNDivLength	147.57052	148.86977	0.67707	
All_MaxFracMatching_Unweighted	116.02174	116.22872	0.02504	
All_MaxMatching_FAMean	80.63155	82.61073	0.66396	
All_MaxMatching_FiberLengthMean	5167.33947	5083.62843	0.31059	
All_MaxMatching_FiberN	2416.37391	2357.39362	0.00037	*
All_MaxMatching_FiberNDivLength	147.14008	148.37032	0.69510	
All_MaxMatching_Unweighted	115.77391	115.96809	0.05570	
All_MinCutBalDivSum_FAMean	0.01998	0.02065	0.71427	
All_MinCutBalDivSum_FiberLengthMean	0.01107	0.01083	0.69973	
All_MinCutBalDivSum_FiberN	0.02507	0.02029	0.00001	*
All_MinCutBalDivSum_FiberNDivLength	0.03425	0.03078	0.12279	
All_MinCutBalDivSum_Unweighted	0.01315	0.01234	0.09039	
All_MinSpanningForest_FAMean	50.81293	47.94001	0.00000	*
All_MinSpanningForest_FiberLengthMean	2794.74279	2822.10418	0.00013	*
All_MinSpanningForest_FiberN	245.53913	245.08511	0.56512	
All_MinSpanningForest_FiberNDivLength	8.05322	8.04386	0.94140	
All_MinVertexCoverBinary_Unweighted	165.60870	166.48936	0.07032	
All_MinVertexCover_FAMean	51.22634	49.27939	0.00000	*
All_MinVertexCover_FiberLengthMean	5170.96696	5072.65831	0.23874	
All_MinVertexCover_FiberN	2424.14348	2360.04787	0.00010	*
All_MinVertexCover_FiberNDivLength	128.48641	128.07573	0.70058	
All_MinVertexCover_Unweighted	116.02609	116.21277	0.04726	
All_PGEigengap_FAMean	0.01891	0.01708	0.00376	*
All_PGEigengap_FiberLengthMean	0.01548	0.01480	0.37661	
All_PGEigengap_FiberN	0.02475	0.02033	0.00000	*
All_PGEigengap_FiberNDivLength	0.02404	0.01916	0.00000	*
All_PGEigengap_Unweighted	0.01757	0.01595	0.00442	*

All_Sum_FAMean	673.67412	617.76979	0.00000	*
All_Sum_FiberLengthMean	50198.24877	47824.57236	0.00472	*
All_Sum_FiberN	13167.07826	12564.14894	0.00000	*
All_Sum_FiberNDivLength	619.73687	597.48943	0.00000	*
All_Sum_Unweighted	1794.95652	1737.55319	0.00000	*
Left_AdjLMaxDivD_FAMean	1.58747	1.61084	0.01155	
Left_AdjLMaxDivD_FiberLengthMean	1.66269	1.66928	0.55075	
Left_AdjLMaxDivD_FiberN	2.55064	2.63591	0.01316	
Left_AdjLMaxDivD_FiberNDivLength	2.46922	2.49502	0.38718	
Left_AdjLMaxDivD_Unweighted	1.42162	1.41012	0.03060	
Left_HoffmanBound_FAMean	4.13962	4.16628	0.29466	
Left_HoffmanBound_FiberLengthMean	3.14236	3.16818	0.33950	
Left_HoffmanBound_FiberN	2.60284	2.59995	0.88033	
Left_HoffmanBound_FiberNDivLength	2.52273	2.50376	0.34043	
Left_HoffmanBound_Unweighted	4.31547	4.30642	0.70557	
Left_LogSpanningForestN_FAMean	161.03690	150.27264	0.00000	*
Left_LogSpanningForestN_FiberLengthMean	664.06115	660.91658	0.17431	
Left_LogSpanningForestN_FiberN	481.98760	479.06065	0.02835	
Left_LogSpanningForestN_FiberNDivLength	130.81017	128.39044	0.03790	
Left_LogSpanningForestN_Unweighted	287.57562	285.21020	0.04173	
Left_MaxFracMatching_FAMean	40.84437	41.80238	0.68549	
Left_MaxFracMatching_FiberLengthMean	2683.08115	2626.73527	0.22816	
Left_MaxFracMatching_FiberN	1199.56522	1194.31383	0.63858	
Left_MaxFracMatching_FiberNDivLength	75.23642	76.01364	0.63792	
Left_MaxFracMatching_Unweighted	59.02174	59.15426	0.02276	
Left_MaxMatching_FAMean	40.73101	41.60035	0.71104	
Left_MaxMatching_FiberLengthMean	2679.39613	2637.73582	0.36598	
Left_MaxMatching_FiberN	1197.97391	1193.95745	0.72028	
Left_MaxMatching_FiberNDivLength	75.00839	75.81179	0.62408	
Left_MaxMatching_Unweighted	58.79130	58.86170	0.20064	
Left_MinCutBalDivSum_FAMean	0.20453	0.21086	0.71731	
Left_MinCutBalDivSum_FiberLengthMean	0.14246	0.12181	0.00000	*
Left_MinCutBalDivSum_FiberN	0.09868	0.08273	0.00000	*
Left_MinCutBalDivSum_FiberNDivLength	0.18665	0.19754	0.62306	
Left_MinCutBalDivSum_Unweighted	0.13857	0.12295	0.00000	*
Left_MinSpanningForest_FAMean	25.19855	23.64144	0.00000	*
Left_MinSpanningForest_FiberLengthMean	1423.68813	1438.50545	0.00028	*
Left_MinSpanningForest_FiberN	127.06957	127.25532	0.86129	
Left_MinSpanningForest_FiberNDivLength	4.18575	4.20175	0.87349	
Left_MinVertexCoverBinary_Unweighted	83.51304	83.96809	0.11146	
Left_MinVertexCover_FAMean	25.57763	24.42983	0.00000	*
Left_MinVertexCover_FiberLengthMean	2683.63258	2628.92733	0.23810	
Left_MinVertexCover_FiberN	1201.44348	1193.03723	0.44260	
Left_MinVertexCover_FiberNDivLength	65.50938	65.48566	0.97350	
Left_MinVertexCover_Unweighted	59.02174	59.14362	0.03941	
Left_PGEigengap_FAMean	0.13999	0.12101	0.00000	*
Left_PGEigengap_FiberLengthMean	0.14328	0.12313	0.00000	*
Left_PGEigengap_FiberN	0.09276	0.07605	0.00000	*
Left_PGEigengap_FiberNDivLength	0.07073	0.05988	0.00000	*
Left_PGEigengap_Unweighted	0.12467	0.10642	0.00000	*

Left_Sum_FAMean	333.37366	304.91149	0.00000	*
Left_Sum_FiberLengthMean	25766.38164	24536.70024	0.00808	*
Left_Sum_FiberN	6538.80000	6291.28723	0.00000	*
Left_Sum_FiberNDivLength	308.66574	299.55206	0.00180	*
Left_Sum_Unweighted	907.06957	880.01064	0.00012	*
Right_AdjLMaxDivD_FAMean	1.54054	1.54133	0.93800	
Right_AdjLMaxDivD_FiberLengthMean	1.63079	1.65634	0.05224	
Right_AdjLMaxDivD_FiberN	2.66812	2.74516	0.06771	
Right_AdjLMaxDivD_FiberNDivLength	2.39111	2.38887	0.93985	
Right_AdjLMaxDivD_Unweighted	1.39936	1.38662	0.04221	
Right_HoffmanBound_FAMean	4.13168	4.12126	0.65194	
Right_HoffmanBound_FiberLengthMean	3.17576	3.22074	0.08033	
Right_HoffmanBound_FiberN	2.53296	2.48305	0.00274	*
Right_HoffmanBound_FiberNDivLength	2.54416	2.47185	0.00005	*
Right_HoffmanBound_Unweighted	4.30307	4.28104	0.31741	
Right_LogSpanningForestN_FAMean	160.17261	151.97412	0.00005	*
Right_LogSpanningForestN_FiberLengthMean	637.98932	634.33567	0.12353	
Right_LogSpanningForestN_FiberN	463.72405	459.96553	0.00579	*
Right_LogSpanningForestN_FiberNDivLength	125.57724	123.36773	0.03373	
Right_LogSpanningForestN_Unweighted	277.44846	274.92442	0.03312	
Right_MaxFracMatching_FAMean	39.83302	40.91191	0.62599	
Right_MaxFracMatching_FiberLengthMean	2475.52017	2429.06018	0.27746	
Right_MaxFracMatching_FiberN	1133.25652	1131.97340	0.90188	
Right_MaxFracMatching_FiberNDivLength	70.27104	72.36800	0.18407	
Right_MaxFracMatching_Unweighted	57.00435	57.07979	0.22364	
Right_MaxMatching_FAMean	39.69325	40.75250	0.63017	
Right_MaxMatching_FiberLengthMean	2472.27779	2429.38282	0.31079	
Right_MaxMatching_FiberN	1131.71304	1127.52128	0.68653	
Right_MaxMatching_FiberNDivLength	70.03999	71.94388	0.22804	
Right_MaxMatching_Unweighted	56.72174	56.82979	0.08738	
Right_MinCutBalDivSum_FAMean	0.19791	0.19350	0.77184	
Right_MinCutBalDivSum_FiberLengthMean	0.14165	0.11868	0.00000	*
Right_MinCutBalDivSum_FiberN	0.09754	0.08410	0.00000	*
Right_MinCutBalDivSum_FiberNDivLength	0.18125	0.18593	0.81709	
Right_MinCutBalDivSum_Unweighted	0.13393	0.11525	0.00000	*
Right_MinSpanningForest_FAMean	25.69248	24.41148	0.00008	*
Right_MinSpanningForest_FiberLengthMean	1365.19318	1377.32416	0.00707	*
Right_MinSpanningForest_FiberN	119.54783	119.06383	0.29718	
Right_MinSpanningForest_FiberNDivLength	3.99147	3.98268	0.89969	
Right_MinVertexCoverBinary_Unweighted	81.69565	82.21277	0.07856	
Right_MinVertexCover_FAMean	25.49721	24.70942	0.00019	*
Right_MinVertexCover_FiberLengthMean	2473.11664	2427.90233	0.29233	
Right_MinVertexCover_FiberN	1133.89565	1131.75532	0.83718	
Right_MinVertexCover_FiberNDivLength	60.96391	62.13464	0.09034	
Right_MinVertexCover_Unweighted	57.00870	57.07447	0.29182	
Right_PGEigengap_FAMean	0.13714	0.11390	0.00000	*
Right_PGEigengap_FiberLengthMean	0.14364	0.11894	0.00000	*
Right_PGEigengap_FiberN	0.09419	0.07578	0.00000	*
Right_PGEigengap_FiberNDivLength	0.07216	0.06037	0.00000	*
Right_PGEigengap_Unweighted	0.12001	0.09968	0.00000	*

Right_Sum_FAMean	330.57089	304.41951	0.00000	*
Right_Sum_FiberLengthMean	23845.34938	22753.02865	0.01223	
Right_Sum_FiberN	6284.90435	6008.05319	0.00000	*
Right_Sum_FiberNDivLength	294.60676	285.84877	0.00046	*
Right_Sum_Unweighted	864.30435	835.94681	0.00005	*

7.5. Table 5

Table 5: In this table, we give the graph-theoretic parameters computed for the 463-vertex graphs. The table contains their arithmetic means in the male and female groups, and the corresponding p-values for group 0 (see the “Statistical analysis” subsection). The graph-parameters and the syntax of the data are defined in the main text. Significant differences ($p < 0.01$) are denoted with an asterisk in the last column.

Property	Female	Male	p-value	
All_AdjLMaxDivD_FAMean	2.15152	2.13711	0.32214	
All_AdjLMaxDivD_FiberLengthMean	2.34498	2.33964	0.79818	
All_AdjLMaxDivD_FiberN	5.17834	5.08521	0.21601	
All_AdjLMaxDivD_FiberNDivLength	5.09639	4.80319	0.00063	*
All_AdjLMaxDivD_Unweighted	1.88865	1.84785	0.00023	*
All_HoffmanBound_FAMean	3.61964	3.63864	0.29281	
All_HoffmanBound_FiberLengthMean	2.92690	2.95102	0.27306	
All_HoffmanBound_FiberN	2.25823	2.26733	0.51416	
All_HoffmanBound_FiberNDivLength	2.22839	2.24269	0.30350	
All_HoffmanBound_Unweighted	3.73096	3.72649	0.81057	
All_LeftRatio_FAMean	0.97770	0.97919	0.75271	
All_LeftRatio_FiberLengthMean	1.01124	1.01629	0.37793	
All_LeftRatio_FiberN	0.99320	1.00153	0.07359	
All_LeftRatio_FiberNDivLength	0.99524	1.00124	0.17321	
All_LeftRatio_Unweighted	1.00145	1.00583	0.24066	
All_LogSpanningForestN_FAMean	438.34886	412.50442	0.00033	*
All_LogSpanningForestN_FiberLengthMean	2305.78858	2315.37932	0.34655	
All_LogSpanningForestN_FiberN	1447.86881	1446.88135	0.85703	
All_LogSpanningForestN_FiberNDivLength	150.36225	143.99520	0.05704	
All_LogSpanningForestN_Unweighted	934.65818	939.07724	0.38738	
All_MaxFracMatching_FAMean	98.71274	96.32183	0.63384	
All_MaxFracMatching_FiberLengthMean	7956.88960	7886.29757	0.56900	
All_MaxFracMatching_FiberN	2429.66522	2363.79787	0.00004	*
All_MaxFracMatching_FiberNDivLength	140.61036	138.76925	0.69162	
All_MaxFracMatching_Unweighted	221.49565	223.32447	0.00011	*
All_MaxMatching_FAMean	98.57616	96.20753	0.63640	
All_MaxMatching_FiberLengthMean	7947.72364	7904.18602	0.72316	
All_MaxMatching_FiberN	2425.98261	2360.14894	0.00003	*
All_MaxMatching_FiberNDivLength	140.13846	138.40665	0.70987	
All_MaxMatching_Unweighted	221.25217	223.14894	0.00006	*
All_MinCutBalDivSum_FAMean	0.01041	0.00969	0.17424	
All_MinCutBalDivSum_FiberLengthMean	0.00811	0.00763	0.28949	
All_MinCutBalDivSum_FiberN	0.02422	0.01949	0.00000	*
All_MinCutBalDivSum_FiberNDivLength	0.02518	0.02013	0.00009	*

All_MinCutBalDivSum_Unweighted	0.00910	0.00828	0.01617	
All_MinSpanningForest_FAMean	97.40278	92.60970	0.00000	*
All_MinSpanningForest_FiberLengthMean	5338.18749	5382.67530	0.00627	*
All_MinSpanningForest_FiberN	479.43478	480.13830	0.65286	
All_MinSpanningForest_FiberNDivLength	18.73746	18.70539	0.88733	
All_MinVertexCoverBinary_Unweighted	274.94783	279.74468	0.00020	*
All_MinVertexCover_FAMean	88.27609	86.05404	0.00196	*
All_MinVertexCover_FiberLengthMean	7960.31876	7887.04893	0.55370	
All_MinVertexCover_FiberN	2430.06957	2363.65426	0.00003	*
All_MinVertexCover_FiberNDivLength	130.90128	129.49926	0.14031	
All_MinVertexCover_Unweighted	221.47826	223.32979	0.00010	*
All_PGEigengap_FAMean	0.01118	0.01018	0.20415	
All_PGEigengap_FiberLengthMean	0.00906	0.00891	0.84118	
All_PGEigengap_FiberN	0.01884	0.01559	0.01070	
All_PGEigengap_FiberNDivLength	0.01752	0.01408	0.00291	*
All_PGEigengap_Unweighted	0.01001	0.00924	0.26355	
All_Sum_FAMean	1011.72390	943.89996	0.00000	*
All_Sum_FiberLengthMean	72818.65816	70226.45899	0.03170	
All_Sum_FiberN	13522.65217	12957.94681	0.00000	*
All_Sum_FiberNDivLength	654.01169	634.54064	0.00004	*
All_Sum_Unweighted	2760.65217	2721.54255	0.06866	
Left_AdjLMaxDivD_FAMean	2.13581	2.13924	0.82156	
Left_AdjLMaxDivD_FiberLengthMean	2.27317	2.26801	0.78357	
Left_AdjLMaxDivD_FiberN	4.06052	4.22036	0.00752	*
Left_AdjLMaxDivD_FiberNDivLength	3.88928	3.92498	0.47520	
Left_AdjLMaxDivD_Unweighted	1.85707	1.81941	0.00037	*
Left_HoffmanBound_FAMean	3.72900	3.78125	0.02704	
Left_HoffmanBound_FiberLengthMean	2.96178	2.98489	0.35233	
Left_HoffmanBound_FiberN	2.50420	2.47733	0.11044	
Left_HoffmanBound_FiberNDivLength	2.46140	2.44273	0.25769	
Left_HoffmanBound_Unweighted	3.82171	3.83488	0.55227	
Left_LogSpanningForestN_FAMean	210.12642	196.40915	0.00019	*
Left_LogSpanningForestN_FiberLengthMean	1151.90236	1159.44304	0.14835	
Left_LogSpanningForestN_FiberN	721.86079	722.81452	0.75427	
Left_LogSpanningForestN_FiberNDivLength	72.52656	69.28217	0.13042	
Left_LogSpanningForestN_Unweighted	464.90819	468.28624	0.20386	
Left_MaxFracMatching_FAMean	48.53975	47.21580	0.60516	
Left_MaxFracMatching_FiberLengthMean	4032.23315	4001.12956	0.64087	
Left_MaxFracMatching_FiberN	1172.41304	1173.14894	0.94108	
Left_MaxFracMatching_FiberNDivLength	69.42651	69.81974	0.86649	
Left_MaxFracMatching_Unweighted	111.02174	112.06915	0.00022	*
Left_MaxMatching_FAMean	48.46705	47.17865	0.61382	
Left_MaxMatching_FiberLengthMean	4029.31001	4012.21426	0.79659	
Left_MaxMatching_FiberN	1168.78261	1172.34043	0.72673	
Left_MaxMatching_FiberNDivLength	69.12320	69.63778	0.82594	
Left_MaxMatching_Unweighted	110.73043	111.80851	0.00011	*
Left_MinCutBalDivSum_FAMean	0.09944	0.08854	0.05366	
Left_MinCutBalDivSum_FiberLengthMean	0.09034	0.07803	0.00002	*
Left_MinCutBalDivSum_FiberN	0.06837	0.05971	0.00000	*
Left_MinCutBalDivSum_FiberNDivLength	0.08119	0.07437	0.51027	

Left_MinCutBalDivSum_Unweighted	0.09033	0.07828	0.00000	*
Left_MinSpanningForest_FAMean	47.42016	44.98209	0.00000	*
Left_MinSpanningForest_FiberLengthMean	2684.63877	2718.61109	0.00029	*
Left_MinSpanningForest_FiberN	242.71304	244.21277	0.26029	
Left_MinSpanningForest_FiberNDivLength	9.52708	9.56275	0.79983	
Left_MinVertexCoverBinary_Unweighted	136.82609	139.48936	0.00028	*
Left_MinVertexCover_FAMean	43.23640	41.95796	0.00078	*
Left_MinVertexCover_FiberLengthMean	4034.19939	4001.84626	0.62665	
Left_MinVertexCover_FiberN	1172.68261	1172.98936	0.97547	
Left_MinVertexCover_FiberNDivLength	64.50611	65.12631	0.31298	
Left_MinVertexCover_Unweighted	111.02174	112.07447	0.00020	*
Left_PGEigengap_FAMean	0.08150	0.06923	0.00319	*
Left_PGEigengap_FiberLengthMean	0.08494	0.07246	0.00663	*
Left_PGEigengap_FiberN	0.06397	0.05295	0.00077	*
Left_PGEigengap_FiberNDivLength	0.04746	0.04080	0.00312	*
Left_PGEigengap_Unweighted	0.07018	0.05920	0.00189	*
Left_Sum_FAMean	494.72731	461.64225	0.00000	*
Left_Sum_FiberLengthMean	36823.20925	35652.14913	0.06912	
Left_Sum_FiberN	6711.51304	6483.65957	0.00001	*
Left_Sum_FiberNDivLength	325.29947	317.66272	0.01038	
Left_Sum_Unweighted	1381.98261	1368.69149	0.24506	
Right_AdjLMaxDivD_FAMean	2.04487	2.02697	0.29333	
Right_AdjLMaxDivD_FiberLengthMean	2.19527	2.21743	0.25616	
Right_AdjLMaxDivD_FiberN	4.29277	4.40447	0.13066	
Right_AdjLMaxDivD_FiberNDivLength	3.85170	3.79705	0.35469	
Right_AdjLMaxDivD_Unweighted	1.80761	1.77132	0.00152	*
Right_HoffmanBound_FAMean	3.62789	3.62380	0.83491	
Right_HoffmanBound_FiberLengthMean	2.96970	2.96886	0.96837	
Right_HoffmanBound_FiberN	2.39859	2.35006	0.00045	*
Right_HoffmanBound_FiberNDivLength	2.45102	2.39300	0.00005	*
Right_HoffmanBound_Unweighted	3.71467	3.70197	0.52197	
Right_LogSpanningForestN_FAMean	222.72004	210.78247	0.00395	*
Right_LogSpanningForestN_FiberLengthMean	1144.69241	1146.71072	0.72684	
Right_LogSpanningForestN_FiberN	717.84406	716.02759	0.58524	
Right_LogSpanningForestN_FiberNDivLength	72.40229	70.05104	0.26626	
Right_LogSpanningForestN_Unweighted	463.53301	464.48221	0.75133	
Right_MaxFracMatching_FAMean	50.04924	48.95794	0.65866	
Right_MaxFracMatching_FiberLengthMean	3910.77231	3870.86335	0.54062	
Right_MaxFracMatching_FiberN	1150.92174	1146.97872	0.70870	
Right_MaxFracMatching_FiberNDivLength	67.80675	68.08738	0.90588	
Right_MaxFracMatching_Unweighted	110.47826	111.23936	0.00309	*
Right_MaxMatching_FAMean	49.96835	48.87203	0.65625	
Right_MaxMatching_FiberLengthMean	3903.73000	3876.11184	0.66742	
Right_MaxMatching_FiberN	1150.87826	1144.00000	0.50989	
Right_MaxMatching_FiberNDivLength	67.68323	67.87734	0.93476	
Right_MaxMatching_Unweighted	110.25217	111.04255	0.00204	*
Right_MinCutBalDivSum_FAMean	0.10508	0.09217	0.01168	
Right_MinCutBalDivSum_FiberLengthMean	0.09559	0.08090	0.00000	*
Right_MinCutBalDivSum_FiberN	0.07388	0.06514	0.00000	*
Right_MinCutBalDivSum_FiberNDivLength	0.08568	0.07909	0.50488	

Right_MinCutBalDivSum_Unweighted	0.09328	0.07967	0.00000	*
Right_MinSpanningForest_FAMean	50.08262	47.75359	0.00005	*
Right_MinSpanningForest_FiberLengthMean	2647.49286	2658.31431	0.26500	
Right_MinSpanningForest_FiberN	238.13043	237.70213	0.67440	
Right_MinSpanningForest_FiberNDivLength	9.35118	9.32215	0.83349	
Right_MinVertexCoverBinary_Unweighted	137.79130	139.92553	0.00346	*
Right_MinVertexCover_FAMean	44.88732	43.91222	0.01455	
Right_MinVertexCover_FiberLengthMean	3912.35409	3870.75981	0.52310	
Right_MinVertexCover_FiberN	1151.06087	1147.00532	0.69964	
Right_MinVertexCover_FiberNDivLength	62.98171	63.52966	0.41129	
Right_MinVertexCover_Unweighted	110.46087	111.23936	0.00259	*
Right_PGEigengap_FAMean	0.08160	0.06725	0.00007	*
Right_PGEigengap_FiberLengthMean	0.08365	0.06956	0.00052	*
Right_PGEigengap_FiberN	0.06575	0.05389	0.00009	*
Right_PGEigengap_FiberNDivLength	0.05081	0.04228	0.00011	*
Right_PGEigengap_Unweighted	0.06961	0.05717	0.00008	*
Right_Sum_FAMean	506.02858	472.91635	0.00000	*
Right_Sum_FiberLengthMean	35355.01763	34004.03695	0.03615	
Right_Sum_FiberN	6466.53913	6209.79787	0.00000	*
Right_Sum_FiberNDivLength	312.21774	304.73958	0.00331	*
Right_Sum_Unweighted	1352.97391	1329.13830	0.05687	

7.6. Table 6

Table 6: In this table, we give the graph-theoretic parameters computed for the 1015-vertex graphs. The table contains their arithmetic means in the male and female groups, and the corresponding p-values for group 0 (see the “Statistical analysis” subsection). The graph-parameters and the syntax of the data are defined in the main text. Significant differences ($p < 0.01$) are denoted with an asterisk in the last column.

Property	Female	Male	p-value	
All_AdjLMaxDivD_FAMean	3.26391	3.21057	0.03613	
All_AdjLMaxDivD_FiberLengthMean	3.60508	3.61334	0.81478	
All_AdjLMaxDivD_FiberN	10.24529	9.92755	0.07190	
All_AdjLMaxDivD_FiberNDivLength	10.08175	9.36632	0.00022	*
All_AdjLMaxDivD_Unweighted	2.81864	2.74618	0.00035	*
All_HoffmanBound_FAMean	3.12681	3.13308	0.67861	
All_HoffmanBound_FiberLengthMean	2.69885	2.72366	0.16335	
All_HoffmanBound_FiberN	2.18923	2.19336	0.71714	
All_HoffmanBound_FiberNDivLength	2.18250	2.19168	0.42770	
All_HoffmanBound_Unweighted	3.15010	3.16902	0.19317	
All_LeftRatio_FAMean	0.98504	0.98697	0.65952	
All_LeftRatio_FiberLengthMean	1.01722	1.02269	0.31705	
All_LeftRatio_FiberN	0.99283	1.00175	0.05057	
All_LeftRatio_FiberNDivLength	0.99580	1.00216	0.13961	
All_LeftRatio_Unweighted	1.00822	1.01172	0.34731	
All_LogSpanningForestN_FAMean	452.66618	401.59076	0.00002	*
All_LogSpanningForestN_FiberLengthMean	3998.62984	4045.89366	0.05608	
All_LogSpanningForestN_FiberN	2105.94128	2112.41461	0.55725	

All_LogSpanningForestN_FiberNDivLength	-350.40752	-376.52817	0.00003	*
All_LogSpanningForestN_Unweighted	1433.48889	1450.08490	0.11718	
All_MaxFracMatching_FAMean	375.55439	381.61057	0.65457	
All_MaxFracMatching_FiberLengthMean	12308.92247	12225.06692	0.65914	
All_MaxFracMatching_FiberN	2506.50877	2427.63298	0.00000	*
All_MaxFracMatching_FiberNDivLength	389.77109	392.09308	0.87595	
All_MaxFracMatching_Unweighted	415.21491	422.88298	0.00017	*
All_MaxMatching_FAMean	375.08500	373.49236	0.91172	
All_MaxMatching_FiberLengthMean	12306.61007	12267.82644	0.83636	
All_MaxMatching_FiberN	2505.11404	2426.30851	0.00000	*
All_MaxMatching_FiberNDivLength	382.10096	389.68108	0.63129	
All_MaxMatching_Unweighted	415.16964	413.96739	0.84640	
All_MinCutBalDivSum_FAMean	0.01274	0.01336	0.59086	
All_MinCutBalDivSum_FiberLengthMean	0.00602	0.00563	0.24543	
All_MinCutBalDivSum_FiberN	0.02374	0.01909	0.00000	*
All_MinCutBalDivSum_FiberNDivLength	0.03720	0.03516	0.51965	
All_MinCutBalDivSum_Unweighted	0.00668	0.00596	0.00518	*
All_MinSpanningForest_FAMean	201.14246	194.00690	0.00010	*
All_MinSpanningForest_FiberLengthMean	10810.54420	10938.08381	0.02244	
All_MinSpanningForest_FiberN	945.42105	957.31915	0.00215	*
All_MinSpanningForest_FiberNDivLength	42.55934	43.50234	0.00901	*
All_MinVertexCoverBinary_Unweighted	452.99123	464.13830	0.00021	*
All_MinVertexCover_FAMean	151.11374	148.75595	0.06900	
All_MinVertexCover_FiberLengthMean	12315.25393	12234.71947	0.67124	
All_MinVertexCover_FiberN	2508.62281	2429.99468	0.00000	*
All_MinVertexCover_FiberNDivLength	138.09749	136.42385	0.08085	
All_MinVertexCover_Unweighted	414.86161	422.88043	0.00009	*
All_PGEigengap_FAMean	0.00055	0.00060	0.84367	
All_PGEigengap_FiberLengthMean	0.00046	0.00056	0.68494	
All_PGEigengap_FiberN	0.00118	0.00120	0.97715	
All_PGEigengap_FiberNDivLength	0.00106	0.00105	0.98422	
All_PGEigengap_Unweighted	0.00049	0.00057	0.75560	
All_Sum_FAMean	1435.45723	1356.82420	0.00001	*
All_Sum_FiberLengthMean	100058.53295	97231.32300	0.07727	
All_Sum_FiberN	13702.51754	13165.47872	0.00000	*
All_Sum_FiberNDivLength	675.08211	658.32175	0.00051	*
All_Sum_Unweighted	3950.33333	3942.51064	0.81017	
Left_AdjLMaxDivD_FAMean	3.18888	3.15430	0.18683	
Left_AdjLMaxDivD_FiberLengthMean	3.45389	3.44831	0.86339	
Left_AdjLMaxDivD_FiberN	7.44018	7.75972	0.00670	*
Left_AdjLMaxDivD_FiberNDivLength	7.25256	7.28578	0.75531	
Left_AdjLMaxDivD_Unweighted	2.73200	2.66542	0.00095	*
Left_HoffmanBound_FAMean	3.18792	3.21815	0.10077	
Left_HoffmanBound_FiberLengthMean	2.72983	2.74135	0.56234	
Left_HoffmanBound_FiberN	2.39551	2.36640	0.05764	
Left_HoffmanBound_FiberNDivLength	2.37202	2.36850	0.80888	
Left_HoffmanBound_Unweighted	3.19577	3.21727	0.20726	
Left_LogSpanningForestN_FAMean	215.74379	190.37937	0.00005	*
Left_LogSpanningForestN_FiberLengthMean	2004.39019	2032.53459	0.03146	
Left_LogSpanningForestN_FiberN	1056.51036	1061.10443	0.46768	

Left_LogSpanningForestN_FiberNDivLength	-172.96633	-186.83057	0.00045	*
Left_LogSpanningForestN_Unweighted	718.69635	728.97009	0.07009	
Left_MaxFracMatching_FAMean	187.79143	190.67012	0.67347	
Left_MaxFracMatching_FiberLengthMean	6248.24855	6224.53571	0.81537	
Left_MaxFracMatching_FiberN	1211.57456	1215.34043	0.71012	
Left_MaxFracMatching_FiberNDivLength	193.58633	196.07530	0.73586	
Left_MaxFracMatching_Unweighted	207.90789	211.61170	0.00118	*
Left_MaxMatching_FAMean	187.56459	190.57398	0.65856	
Left_MaxMatching_FiberLengthMean	6246.36085	6246.80376	0.99648	
Left_MaxMatching_FiberN	1209.53509	1215.35106	0.56905	
Left_MaxMatching_FiberNDivLength	193.23385	195.74463	0.73407	
Left_MaxMatching_Unweighted	207.66667	211.58511	0.00055	*
Left_MinCutBalDivSum_FAMean	0.10408	0.10872	0.59997	
Left_MinCutBalDivSum_FiberLengthMean	0.05439	0.04836	0.00197	*
Left_MinCutBalDivSum_FiberN	0.04626	0.04202	0.00107	*
Left_MinCutBalDivSum_FiberNDivLength	0.21596	0.21436	0.94069	
Left_MinCutBalDivSum_Unweighted	0.05508	0.04783	0.00000	*
Left_MinSpanningForest_FAMean	97.84281	94.20558	0.00024	*
Left_MinSpanningForest_FiberLengthMean	5420.46856	5493.47367	0.01596	
Left_MinSpanningForest_FiberN	477.09649	483.20213	0.02006	
Left_MinSpanningForest_FiberNDivLength	21.48953	21.86841	0.08025	
Left_MinVertexCoverBinary_Unweighted	226.83333	232.63830	0.00034	*
Left_MinVertexCover_FAMean	74.33023	73.06766	0.06543	
Left_MinVertexCover_FiberLengthMean	6247.30024	6226.93453	0.84176	
Left_MinVertexCover_FiberN	1211.01316	1215.39894	0.65766	
Left_MinVertexCover_FiberNDivLength	68.29763	69.18052	0.16165	
Left_MinVertexCover_Unweighted	207.92982	211.65426	0.00104	*
Left_PGEigengap_FAMean	0.01291	0.01737	0.18451	
Left_PGEigengap_FiberLengthMean	0.01368	0.01822	0.20492	
Left_PGEigengap_FiberN	0.01193	0.01555	0.23713	
Left_PGEigengap_FiberNDivLength	0.00882	0.01175	0.19242	
Left_PGEigengap_Unweighted	0.01113	0.01460	0.22351	
Left_Sum_FAMean	706.86641	668.88465	0.00003	*
Left_Sum_FiberLengthMean	50905.16818	49686.48356	0.15828	
Left_Sum_FiberN	6797.47368	6589.18085	0.00006	*
Left_Sum_FiberNDivLength	335.85385	329.89072	0.04884	
Left_Sum_Unweighted	1989.76316	1994.22340	0.80307	
Right_AdjLMaxDivD_FAMean	3.13638	3.09093	0.11113	
Right_AdjLMaxDivD_FiberLengthMean	3.44271	3.49144	0.14483	
Right_AdjLMaxDivD_FiberN	7.87548	8.10827	0.10424	
Right_AdjLMaxDivD_FiberNDivLength	7.21299	7.11027	0.38977	
Right_AdjLMaxDivD_Unweighted	2.73516	2.66649	0.00147	*
Right_HoffmanBound_FAMean	3.12011	3.12021	0.99541	
Right_HoffmanBound_FiberLengthMean	2.72047	2.71627	0.80239	
Right_HoffmanBound_FiberN	2.32392	2.27174	0.00008	*
Right_HoffmanBound_FiberNDivLength	2.36632	2.30960	0.00001	*
Right_HoffmanBound_Unweighted	3.13240	3.14164	0.55805	
Right_LogSpanningForestN_FAMean	230.00215	205.04675	0.00017	*
Right_LogSpanningForestN_FiberLengthMean	1983.76491	2002.58051	0.15642	
Right_LogSpanningForestN_FiberN	1040.41771	1041.86173	0.81878	

Right_LogSpanningForestN_FiberNDivLength	-183.37842	-194.97616	0.00128	*
Right_LogSpanningForestN_Unweighted	707.75289	713.51596	0.32314	
Right_MaxFracMatching_FAMean	187.58059	190.72286	0.64031	
Right_MaxFracMatching_FiberLengthMean	6042.45994	5986.31966	0.56896	
Right_MaxFracMatching_FiberN	1183.68860	1167.45213	0.07792	
Right_MaxFracMatching_FiberNDivLength	192.17256	194.82239	0.72256	
Right_MaxFracMatching_Unweighted	207.22368	211.03191	0.00048	*
Right_MaxMatching_FAMean	187.38097	190.51859	0.63955	
Right_MaxMatching_FiberLengthMean	6043.98429	6006.54168	0.70074	
Right_MaxMatching_FiberN	1184.21930	1166.60638	0.05839	
Right_MaxMatching_FiberNDivLength	191.91345	194.56752	0.72161	
Right_MaxMatching_Unweighted	207.02632	211.02128	0.00023	*
Right_MinCutBalDivSum_FAMean	0.10814	0.11038	0.80060	
Right_MinCutBalDivSum_FiberLengthMean	0.05818	0.05098	0.00006	*
Right_MinCutBalDivSum_FiberN	0.04803	0.04336	0.00001	*
Right_MinCutBalDivSum_FiberNDivLength	0.23186	0.22678	0.82294	
Right_MinCutBalDivSum_Unweighted	0.05872	0.05119	0.00000	*
Right_MinSpanningForest_FAMean	103.42417	99.90568	0.00063	*
Right_MinSpanningForest_FiberLengthMean	5384.31437	5439.30295	0.07352	
Right_MinSpanningForest_FiberN	471.37719	478.13830	0.00337	*
Right_MinSpanningForest_FiberNDivLength	21.28508	21.93744	0.00392	*
Right_MinVertexCoverBinary_Unweighted	225.98246	231.21277	0.00179	*
Right_MinVertexCover_FAMean	76.57533	75.67481	0.20158	
Right_MinVertexCover_FiberLengthMean	6050.51258	5994.51322	0.56911	
Right_MinVertexCover_FiberN	1185.97807	1169.50000	0.07615	
Right_MinVertexCover_FiberNDivLength	66.21118	66.27928	0.90881	
Right_MinVertexCover_Unweighted	207.20614	211.31915	0.00018	*
Right_PGEigengap_FAMean	0.01491	0.00973	0.11019	
Right_PGEigengap_FiberLengthMean	0.01571	0.00988	0.08719	
Right_PGEigengap_FiberN	0.01257	0.00820	0.11014	
Right_PGEigengap_FiberNDivLength	0.00965	0.00642	0.12520	
Right_PGEigengap_Unweighted	0.01268	0.00812	0.09616	
Right_Sum_FAMean	716.58340	678.16757	0.00005	*
Right_Sum_FiberLengthMean	48496.80981	46948.77164	0.06732	
Right_Sum_FiberN	6560.14035	6312.01064	0.00000	*
Right_Sum_FiberNDivLength	322.67446	316.28095	0.01331	
Right_Sum_Unweighted	1933.52632	1922.39362	0.53559	